ALPHA FOUNDATION FOR THE IMPROVEMENT OF MINE SAFETY AND HEALTH

Final Technical Report

Project Title: "Removal of DPM, silica, and coal dust using high volume fog generation"
Grant Number: AFC316-42
Organization: Clemson University
Principal Investigator: Dr. John R. Saylor
Contact Information : jsaylor@clemson.edu, (864) 656-5621 (v) (864) 656-4435 (fax).
Period of Performance: January 1, 2019 – April 13, 2020.

Acknowledgement/Disclaimer: "This study was sponsored by the Alpha Foundation for the Improvement of Mine Safety and Health, Inc. (ALPHA FOUNDATION). The views, opinions and recommendations expressed herein are solely those of the authors and do not imply any endorsement by the ALPHA FOUNDATION, its Directors and staff."

1.0 Executive Summary (recommended length 1 page): The executive summary should provide a succinct and accurate description of the problem statement, the research approach, accomplishments and expected impact on mining health and safety. Since this executive summary may be released to the general public, budgetary information should not be included.

Problem Statement: The problem that was addressed in this project concerns the elevated risk of respiratory illness that exists for the mining work force caused by exposure to airborne particles in the mining environment. In particular, diesel particulate matter (DPM) is a growing threat to worker health in metal/nonmetal mines where more than 18,000 miners work in approximately 200 underground mines (Monforton, 2006). DPM is a significant concern since the particles formed are virtually all submicron in size and easily penetrate into the lung. Furthermore, DPM particles reside in the mining environment for long periods due to an

essentially zero settling velocity (Bugarski et al., 2012). DPM has been classified as a known human carcinogen (International Agency for Cancer Research, 2012) and chronic exposure increases the risk of cardiovascular, cardiopulmonary, and respiratory disease (OSHA - HA-3590-2012). Evidence continues to accumulate suggesting that diesel exhaust in general and DPM in particular increase the risk of cancer (Garshick, 2004). Because DPM is mostly confined to nanoscale particle diameters, methods for removing it from vehicular exhaust are challenging, since the particles have virtually no inertia at these small diameters. Hence, standard filtration or impaction methods for particle removal are not effective. Accordingly, effective removal of DPM and other nanoparticles must rely on the diffusive motion of these small particles. Since the characteristic length of diffusion tends to be small for the time scales of a particle traveling through a finite sized scavenging system, the overall process of removing nanoparticles can be problematic.

Research Approach: As noted above, diffusion is the process that must be relied upon to remove nanoparticles in diesel exhaust. The characteristic length of a diffusing nanoparticle would be small for the time scales of a particle traveling through a scrubber or filtration system. To address this issue, we sought to reduce the distance such a nanoparticle would have to diffuse by adding fog to the exhaust stream. Specifically, the research approach was to force the diesel exhaust to combine with a high number density of 5 um fog drops. In this way, the nanometer particles only need to diffuse the relatively short distance to a drop. Once this has occurred, removal of the fog drop results in removal of the nanoparticle. And, since 5um drops having significant inertia (compared to the much smaller DPM nanoparticles) they are relatively straightforward to remove via an impactor, a cyclone, or even via gravitational settling.

Accomplishments: During the course of this project, the efficacy of fog in removal of nanoparticles was demonstrated in two setting (i) a laboratory setting, and (ii) and engine test-cell environment. In the laboratory, nanoparticles were generated by the atomization of a solution of sodium dodecyl sulfate (SDS). These nanoparticles were flowed into a fogging chamber where ultrasonic foggers were used to generate fog drops having a nominal diameter of 5um. Experiments demonstrated significant improvement of nanoparticle scavenging by fog, for nanoparticles ranging in from 11 nm to 365 nm in diameter. In the engine test cell environment, similar results were obtained. Again 5um fog drops were generated using ultrasonic transducers and these were shown to increase the scavenging of DPM nanoparticles in the 11 nm to 365 nm range. In the laboratory, scavenging was quantified as a function of the air flow rate, water consumption rate, and particle diameter. In the engine test-cell environment, scavenging of DPM was quantified in terms of particle diameter and engine load. In the engine test-cell environment, significant engineering challenges were identified and addressed, including maintenance of fog generation even as organic films formed on the water surface in the fogging chamber.

Expected Impact on Mining Health and Safety: If implemented in the mining environment, the use of a fog scrubber to remove DPM could have a significant impact on the respiratory health of the mining work force. The approach uses only water and foggers that generate fog using ultrasonic transducers. In the engine studies, the exhaust flow was due to the engine itself. Hence a zero moving parts strategy (or perhaps one moving part if one considers the PZT disc in the foggers to be a moving part) can be implemented that reduces DPM levels.

2.0 Problem Statement and Objective: The solicitation focus area should be identified and the problem statement summarized. Sufficient background information should be provided to justify why this approach is needed to advance the solution to this problem area. The specific aims and research objectives should be clearly documented.

The solicitation focus area was ***Health and Safety Interventions***. The priority area was 1.1: ***Respirable Dust***.

<u>Summary of Problem Statement:</u> The mine health problem that was addressed is the continuing high levels of particulates in the mining environment, specifically the nanoparticles found in diesel exhaust: diesel particulate matter (DPM). It is notable that: (1) there is an enormous degree of exposure to DPM in the metal/nonmetal mining workforce, (2) there is an enormous opportunity to dramatically improve DPM levels in mines due to the highly localized nature of how it is introduced in mines (only from tailpipes), and (3) the threat to the mining workforce by DPM is significant. DPM has been classified as a suspected carcinogen (NIOSH, 1988) and is associated with a variety of acute health effects such as respiratory irritation and nausea (EPA, 2002; Ristovski et al., 2012). DPM exposures can occur in any occupation where diesel equipment is used, particularly when ventilation is insufficient or exhaust after-treatment technologies (e.g., diesel particulate filters, discussed further below) are not used. While underground miners are generally considered to be at highest risk for DPM exposures, surface miners and processing and auxiliary operations workers are also at risk. DPM is a growing concern in metal/nonmetal mines where more than 18,000 miners work in approximately 200 underground mines (Monforton, 2006). Although diesel engines are used less in coal mines, the use of diesels in outby areas is significant and presents a risk to coal mine workers as well. DPM is a significant concern since the particles formed are virtually all submicron in size and easily penetrate into the lung. Furthermore, DPM particles reside in the mining environment for long periods due to an essentially zero settling velocity (Bugarski et al., 2012). DPM has been classified as a known human carcinogen (International Agency for Cancer Research, 2012) and chronic exposure increases the risk of cardiovascular, cardiopulmonary, and respiratory disease (OSHA - HA-3590-2012). Evidence continues to accumulate suggesting that diesel exhaust in general and DPM in particular increase the risk of cancer (Garshick, 2004). Although exhaust after-treatments such as diesel particle filters (DPF) can be effective in removing DPM, challenges remain with this technology with regard to regeneration, maintenance, and other factors.

Summarizing, the health problems posed by DPM in mines is significant, and extant methods for its removal suffer from a range of problems, as is further demonstrated below.

<u>Background Information</u>: Diesel engines are used in a very large number of underground mines. Bugarski et al. (2012) note that according to MSHA, roughly 4800 diesel engines are used in 145 underground coal mines in the United States and that as many as 7700 diesel engines are used in 177 metal/nonmetal mines. In total, as many as 30,000 underground miners may be exposed to high concentrations of DPM due to these diesels (Mischler & Colinet, 2009). The DPM emitted by these engines is a complicated mixture of solid carbon particles, ash, volatile organics, and sulfur containing compounds (Kittelson, 1998). Though the

constituents and relative concentrations of the particles in diesel exhaust vary in a complicated fashion as they evolve from the moment of combustion onward through the exhaust system and into the mining environment, it is clear that DPM is deleterious to human health.

A significant characteristic of DPM is that the particles reside almost exclusively in the submicron range of particle diameters. This is shown in Fig. 1, which is a particle size distribution for the exhaust of a typical diesel engine. This figure shows that in terms of both mass density and number density, virtually all DPM is less than a micron in diameter. In terms of mass, most particles reside between 100nm and 1um, while in terms of number of particles, most DPM resides in the diameter range <50nm. All of these small, submicron particles are cause for concern, since penetration into the human lung increases with decreasing particle diameter (ICRP, 1984).

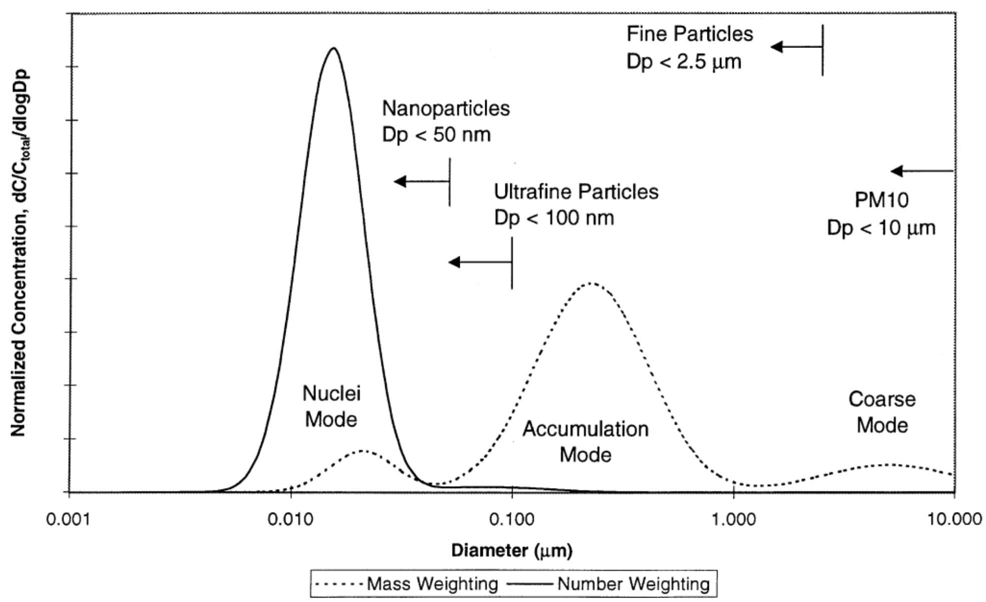

Figure 1: Particle size distribution for a typical diesel engine. Both the number weighting and mass weighting are shown. Plot taken from Kittelson (1998).

Regulations on permissible DPM levels have been implemented for both underground coal mines (30 CFR 72.520, 2001) and metal/nonmetal underground mines (30 CFR 57.5060, 2008). The latter limits personal exposure to less than 160 ug/m^3 total carbon, and is a mass-based method which samples submicron particles. One method for achieving these levels is via mine ventilation. This approach is perhaps the most straightforward since ventilation systems are, of course, already used in underground mines to remove other particulates as well as to reduce to required levels gases such as CO, CO_2, NOx and SOx. However, reduction of DPM to levels that meet regulations requires significant increases in ventilation flow rates beyond that which is necessary to control the levels of these harmful gasses (Schnakenberg & Bugarski, 2002). Hence, the use of ventilation to control DPM levels is an expensive route, and the potential for future regulations on DPM only stands to increase this cost. The other method for reducing DPM levels is to address the problem at the source, namely at the engine or tailpipe. In this category, methods for DPM reduction include use of alternative fuels, operation of the engine in such a way as to reduce DPM emission, the use of diesel particle filters (DPF) and the use of diesel oxidation catalytic converters (DOCC), (Schnakenberg & Bugarski, 2002). These approaches are now surveyed.

Changes in how a diesel engine is operated can result in some reductions in DPM emissions. For example derating, the process of running an engine at reduced power, can reduce DPM by significant amounts. In one study, reductions of as much as 80% by mass for a 4 hp reduction were observed, though more typical numbers are on the order of 50% (Schnakenberg & Bugarski, 2002). Another example of reducing DPM emissions via alternative operating methods is the use of alternate fuels such as biodiesel or diesel combined with water emulsions. Reduction in DPM has been reported in the use of biodiesels. The range in quoted reductions is large, not surprisingly, given the different types of biodiesel blends which are available, not to mention differences in the type of "pure" diesel which can be used as the control case. For example, a 50% reduction was found by Howell & Weber (1977) while only a 20% reduction was observed in a not dissimilar study by Watts et al. (1998). The addition of water in the form of an emulsion has been used to control diesel emissions where reductions in gas phase emissions is the primary benefit, though some reductions in particulate emissions have also been observed (Bugarski, 2011). Also in this category are low sulfur fuels which dramatically reduce the formation of sulfuric acid aerosols, which can be in the nanoparticle range. Methods that eliminate DPM particles once they've been formed include catalysis and filtration. Diesel oxide catalytic converters (DOCC) are used with diesel engines primarily to reduce carbon monoxide and hydrocarbon emissions by oxidizing them to carbon dioxide and water (Bugarski et al., 2011). However DOCCs also reduce DPM and have been shown to result in reductions of 20% - 35% (EPA, 2009; Bugarski et al., 2011). With regard to DPM reductions, diesel particle filters (DPF) are arguably the most effective in DPM mass reduction. DPFs are fine porous filters typically composed of materials such as silicon carbide or ceramic oxide which capture particles in the porous structure. The captured DPM is subsequently eliminated through a regeneration process where the filter temperature is elevated to burn off the DPM cake. This can be done using exhaust heat, via electrical heating, or by removing the filter and regenerating it in an off-site kiln. The effectiveness, on a mass basis, of these filters can be quite high, approaching 99% under proper conditions (Bugarski et al., 2011).

The above survey of extant methods for DPM reductions seems to suggest that the mine operator has numerous tools available, each of which show the potential for significant reduction in DPM levels. Many of the above methods indicate very significant reductions in DPM, perhaps the best being due to DPFs. However caution must be exercised when interpreting quoted percent reductions in DPM for several reasons. First, virtually all of the percent reductions described above are mass based results, which are highly skewed toward larger particles. This is a real concern since, as will be shown below, there is significant evidence to suggest that it is the **number** of particles and not necessarily the **mass** of particles in the nanometer range which impacts human health. Hence, if the reduction in DPM mass due to any of the techniques described above is due primarily, say, to particle reductions in the 100nm - 1.0um range, it could be the case that enormous numbers of particles in the 1nm-10nm range may not be removed at all. One way to illustrate the significance of this point is to simply note that it takes one million particles having a diameter of 1 nm to equal the mass of a single 100nm particle. There is significant evidence to suggest that DPFs and other after-treatment methods are removing mostly "large" nanoparticles (those in the accumulation region), while not affecting, or perhaps even increasing, the number concentration of smaller nanoparticles in the nucleation region (<50nm) range. For example, Dementhon & Martin (1997) showed that nuclei mode DPM was created by DPFs during some loading conditions for a 1.9L VW TDI engine and that nuclei mode particles were generated during regeneration for all cases studied. Vaaraslahti et al. (2004) showed that for a heavy duty diesel operating with a continuously regenerating DPF, nucleation mode particles were significantly reduced, but only at low engine loads and that at high engine loads, the formation of nucleating mode nanoparticles was actually higher with the DPF in place, increasing by over two orders of magnitude in number density at a diameter of 10nm. Maricq et al. (2002) observed a similar effect on a light duty diesel truck, but only when using high sulfur fuel, as did Vogt et al. (2003) in studies of the exhaust plume of a diesel passenger car, as sampled by a chase vehicle. Kittelson et al. (2006) showed a two orders of magnitude increase in 10nm nucleation mode particles when a Continuously Regenerating Trap was used when compared to the uncontrolled exhaust case for a Volvo 6 cylinder, 12 L diesel engine, and Bugarski et al. (2009) found a similar result on an Isuzu C240 light duty diesel in an underground mining environment. Other studies showing an increase or lack of a decrease in nucleation mode nanoparticles when using DPFs exist in the literature, and a good survey can be found in Bugarski et al. (2012).

In medical science, the effect of a substance on human health is typically characterized in a mass-based way. Whether the substance is a drug designed to promote health, or a toxin known to result in morbidity, the figure of merit is typically mass of the compound per unit mass of body weight. However, as noted by Ristovski et al. (2012), particles in general, and nanoparticles in particular cause damage that is not well-correlated to mass. Rather, it is the number concentration (Pope et al., 1995; Dockery et al., 1993) or perhaps the total particle surface area (Oberdorster et al., 2005, 2007) that best correlates DPM toxicity. Indeed, studies have shown that as the particle diameter descends into the 10's of nanometers, materials that are understood to be benign and nonreactive in animal tissue, become toxic. This was shown to be the case for titanium dioxide particles by Seaton et al. (1995) and for Teflon particles by Warheit et al. (1990). Furthermore, at these very small diameters, particles, instead of embedding themselves in the alveolar tissue and relegating their damage only to the lung, can actually translocate to other organs such as the liver, spleen, or brain. This was shown to be the case in animal studies by Elder et al. (2006) and Oberdorster et al. (2004).

In addition to the observation that DPM reductions reported in the literature are mass-based and do not account for the number density effect on health, it should also be noted that even if reductions in number density were comparable to those quoted on a mass basis, reductions, even as large as, say, 90% may not be as significant as they appear. The enormous number densities of nanoparticles in diesel exhaust may mean that levels are still high even when number densities are reduced by a large amount. For example, DPM emissions of an untreated engine tend to reside in the 10^9/cc range, meaning that even a 90% reduction leaves a concentration of 10^8/cc, which is still very large.

Finally, it is noted that the various technologies described above cannot always be used in an additive or multiplicative way to remove diesel emissions. In other words, some technologies help in reducing one aspect of diesel emission, while negatively impacting the ability to remove another part of diesel emission. Perhaps the best known example of this is the NOx/DPM tradeoff which results from the fact that NOx formation increases with combustion temperature, while the opposite is true for DPM (Bugarski et al., 2011).

All of the above indicates that implementation of some or all of the strategies described above may be good approaches for reducing overall DPM levels of large particles. And, given how DPM levels area currently quantified it may be the case that existing technologies are all that is necessary to bring a mine operation into compliance. However, it may very well be the case that future regulations borne from a growing understanding of the health threats associated with nanoparticles that contribute negligibly to overall DPM mass, but are large in number, may require significantly different approaches to DPM removal. Furthermore, given that many of the methods described above are already problematic in various mine conditions, require diligent protocols and maintenance procedures, and/or benefit reductions in one type of DPM emission at the expense of another, exploration of alternative DPM control methods is clearly needed.

The research presented below implements the use of very small water drops, fogs, to eliminate particles. The challenge in removing submicron particles from air is that the particles have very little inertia which is one method by which filters, scrubbers, etc. remove particles. However, as the particle diameter decreases, the effective diffusivity of a particle increases. This allows for the possibility of particle elimination via diffusion toward a collector, such as a filter. However, even for very small particles, the diffusion distance for a particle can be relatively small over the time scales inherent in a typical exhaust system. But this limitation can be overcome if the collector is a fog drop, and if the number density of the fog is large enough that the interdrop spacing is comparable to the particle diffusion distance. It is tempting to compare this approach to that of a wet scrubber – the approach seems to be similar in that drops are used in a gas flow to eliminate an undesirable component. However, wet scrubbers tend to rely on inertia as well, spraying drops downward so that particles will strike the drop surface. That is not the approach in the research described here, where diffusion of particles to drops, both of which are traveling at the same speed as the other is the means by which particles are captured by the drops.

<u>Specific Aims and Research Objectives:</u> The specific aims of this research were to develop a new method for removing nanoparticles that can complement (or perhaps replace) existing approaches such as diesel particulate filters or catalysis-based approaches and which is effective on particle diameters that extend down into the DPM nucleation regime (10nm - 50nm), but is also effective for larger particle diameters, extending well into the micron scale regime. We refer to the device that we have developed as a "fog scrubber" since it combines particles and a high number density of fog drops in one location where they are combined and are subsequently removed as a water stream via a cyclone separator. The fog scrubber operates via a combination of diffusive transport from particles to drops and then inertial transport from the drops to the walls of the cyclone separator. This approach is not chemistry-based and is instead based on purely mechanical mechanisms. Hence particle removal occurs in a way that depends on the particle and drop size and density and does not require a specific chemical environment. In this way, variations in engine type, fuel, operating condition and after-treatment doesn't change the effectiveness of the proposed method. As will be shown below, we have demonstrated the method in a laboratory and engine test-cell environment. In both cases a stream of polluted gas (in the laboratory results, the "pollutant" is not DPM, but sodium dodecyl sulfate) emanating from a pipe is combined with a high number density fog in a fogging chamber. This approach is ideally suited for cleaning diesel

exhaust, since the exhaust emanates from the tailpipe of a vehicle and is therefore eminently suited to directly couple with the fog scrubber.

The ultimate outcome of the proposed study was to have a particle scrubber mounted on a diesel mining vehicle and on a stationary diesel engine in a mining environment. While this was not achieved, what was done was to show that (i) the fog scrubber works in a laboratory environment, and (ii) that the fog scrubber increases DPM removal for a small diesel engine in a controlled engine test cell.

The fog scrubber developed and investigated in this work should enable significantly improved removal of particles ranging from 10nm to tens of microns. This addresses the Respirable Dust priority area.

3.0 Research Approach: The strategy and study design used to solve the problem should be clearly described. The specific tasks that were used to address the research objectives are to be identified and described to a level of detail that would allow another researcher to understand the methodology and experimental design used to achieve the research objectives.

Broadly stated, the research approach was to quantify the performance of the drop scrubber in (1) a laboratory environment where proxy-particles (not DPM) were generated in a controlled environment; (2) to quantify the performance of the drop scrubber in an engine test-cell environment where DPM particles were scrubbed from the exhaust and where the load on the engine was varied; (3) to quantify the performance of the drop scrubber mounted on the tailpipe of a mining vehicle in a mining environment. The strategy was to conduct these tasks in order, since these proceeded from situations where the system was easiest to control to situations where the system was most difficult to control. The first two tasks were completed during the course of the grant period.

Laboratory Environment Experiments

The overall approach for the laboratory tests was to construct the fogger setup and quantify its performance in a laboratory where many of the parameters which are difficult to control in an engine are easily controlled. For example, when operating using diesel engine exhaust, temperature of the flow, particle number density, and overall flow rate are difficult to "set" to specific values. Moreover, in diesel exhaust the chemical makeup of the particles, as well as their diameter, may vary as they flow through the system as they change temperature and as hydrocarbons evaporate or condense. This introduces irreproducibility in the testing environment. In the laboratory setup, the stability of the particles is easy to ensure while flow rates, temperatures, etc. can also be set and held to stable values.

A schematic of the laboratory setup is presented in Figure 2 and Figure 3, below. The first of these shows the portion of the setup used to generate nanoparticles. The approach was to create a solution of sodium dodecyl sulfate (SDS), a detergent which was atomized using the atomizer shown in the figure (TSI, 9302, Single Jet Atomizer). The atomizer generated a range of drop diameters centered at 1.5 um. The SDS solution varied in concentration from 0.15 to

0.36 mg/ml. The key was to ensure that the SDS particles created by the evaporated atomizer drops populated the diameter range that the NanoScan particle counters were sensitive to (11.5 nm – 365 nm). The pressure applied to the atomizer and SDS concentration were adjusted from run to run to ensure this was the case. Upon atomization, the air flowing through the atomizer was directed through two diffusion dryers (ATI, DD-250) to ensure drying of the SDS particles. The compressed air used to drive the flow was house air which had a nominal relative humidity of 5%, hence this also contributed to drying the SDS particles. The dried particles were then passed through a Kr-85 Neutralizer (TSI 3012) to remove residual charge after evaporation.

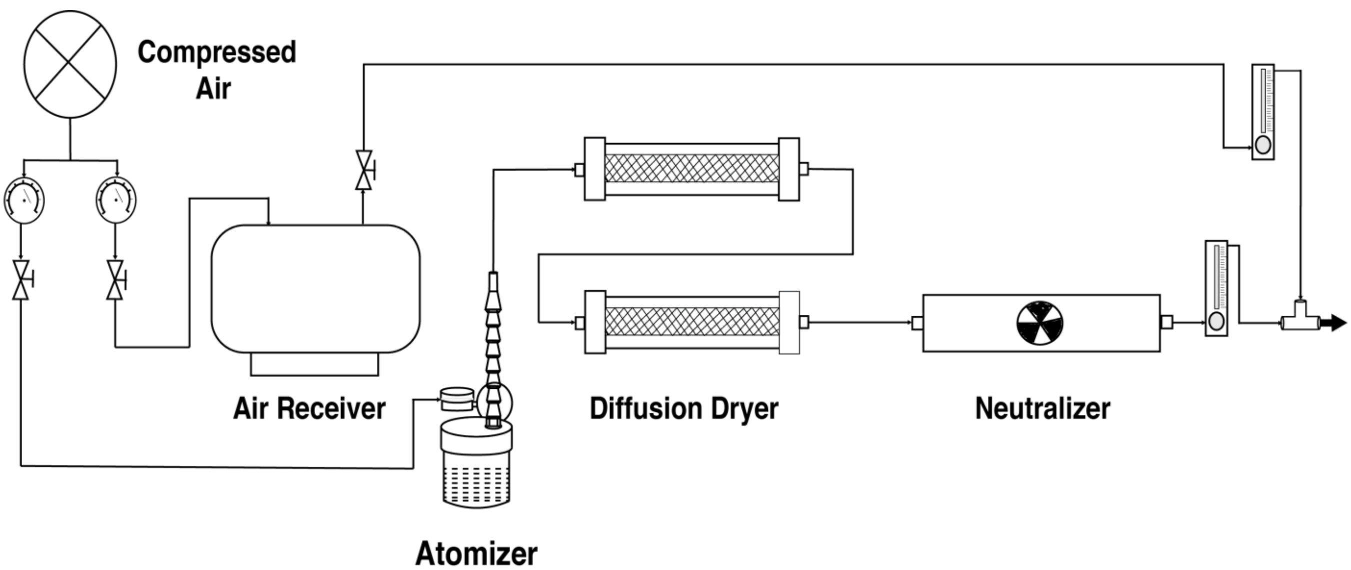

Figure 2- Experimental setup used to generate flow of nanoparticles comprised of SDS. The outlet of this setup is the inlet into the setup presented in Figure 3.

As Figure 2 shows, the resulting particle-laden flow that leaves the particle generation system comes from two air flows, the lower part of the figure shows the portion of the flow where particles are generated. This is combined with the majority of the flow in the upper part of the figure. This portion of the flow goes through a large accumulator tank (75.7 liters) which was installed to damp any pressure oscillations that might exist in the house air source. A total of four air flow rates were explored: 5, 10, 15, and 20 LPM. These values are the sum of the two flows shown in Figure 2 which are combined at the indicated T-junction prior to entering the scavenging apparatus proper, shown in Figure 3.

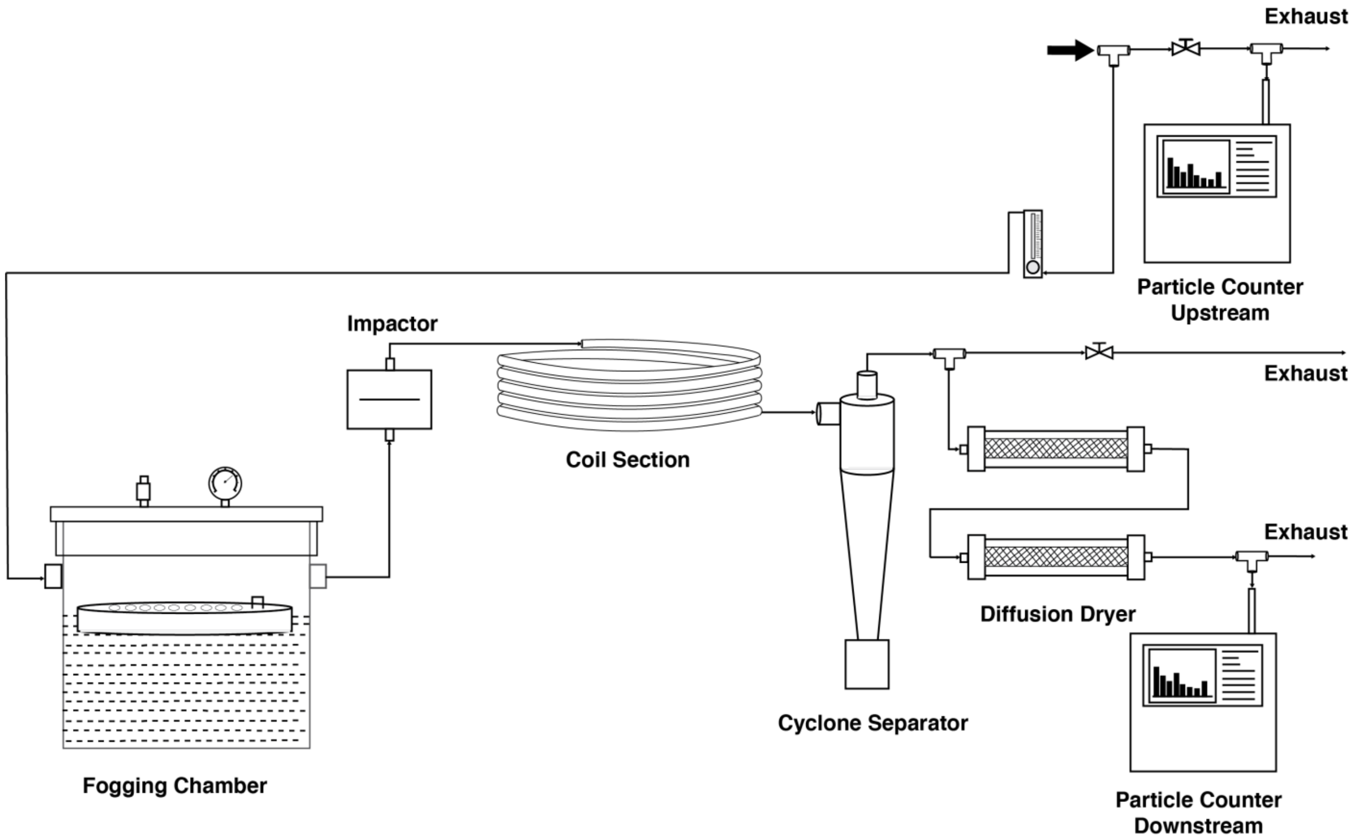

Figure 3- Experimental setup for investigating nanoparticle scavenging in the laboratory environment.

The black arrow in Figure 3 shows where the particle-laden flow from the particle generation setup illustrated in Figure 2 enters the scavenging apparatus. A fraction of the flow is sampled by the first NanoScan (TSI NanoScan SMPS Nanoparticle Sizer 3910) and then is directed to the fogging chamber which was an acrylic box of dimensions 12"x12"x8"(LxWxH), fitted with a pressure gage and pressure relief valve. The fogging chamber was partially filled with doubly distilled water. Significant cleaning protocols were developed to ensure that the fog drops generated in the fogging chamber did not themselves generate nanoparticles once evaporated. Check experiments were periodically run to ensure that the total number of particles generated by running the apparatus without the SDS particle generation unit (i.e. with the atomizer shown in Figure 2 unpressurized) was less than 1000/cc. A 12-disc fogger was used to generate the fog. A rough control of the fog generation rate was obtained by regulating the input voltage. These foggers were placed within a floating circular ring whose center was submerged a fixed distance beneath the water surface at which maximum fog generation occurred.

When the foggers were operating, the fog chamber and the outlet tube from the chamber would accumulate water which would create larger droplets as the air flowed through. Since the goal was to focus on the effect of fog drops on nanoparticle removal (and not any possible effect of these larger drops), an impactor was installed downstream (and in an elevated position) of the fogging chamber to ensure that they were returned to the fogging chamber and did not continue further downstream. The impactor was designed to have a

50% diameter cutoff value of d_{50} = 100um and had dimensions 6.5"x4.5"x3.75" (LxWxH). After the impactor, the flow went through a coil comprised of plastic having an internal diameter of 1.0" and a length of 228". This was included to permit a period of time for particles to diffuse to the fog drops. The tubing was coiled in order to take up less space on the laboratory bench. Following the tube was a cyclone separator designed to remove the drops created by the fogger. A portion of the cyclone output was sampled by the second NanoScan, while the rest of the flow was exhausted to a laboratory vent. The flow sampled by the NanoScan was first passed through two more diffusion dryers (ATI, DD-250) so that drops were not introduced, nor measure by that NanoScan.

A note on measurement philosophy should be made here. From an occupational health perspective, the use of these diffusion dryers implies a conservative mode of measurement. Specifically, their use indicates that we consider a nanoparticle to be scavenged if and only if two things occur. First, the nanoparticle diffuses to a fog drop, and second the fog drop is removed from the flow. Drops which have removed nanoparticles but remain in the flow will evaporate in the diffusion dryer after which the nanoparticle will be released and presumably measured by the NanoScan – *viz.* it will be counted and therefore considered an *unscavenged* drop. In an actual industrial environment, a nanoparticle that attaches to a 5 um fog drop that remains in the air, though less desirable than such a drop which is removed, still improves the environment, since micron-scale fog drops may be removed in the oropharyngeal region of the human anatomy and likely will not make it to the deepest recesses of the lungs. All of this is to say that our measurement approach is conservative.

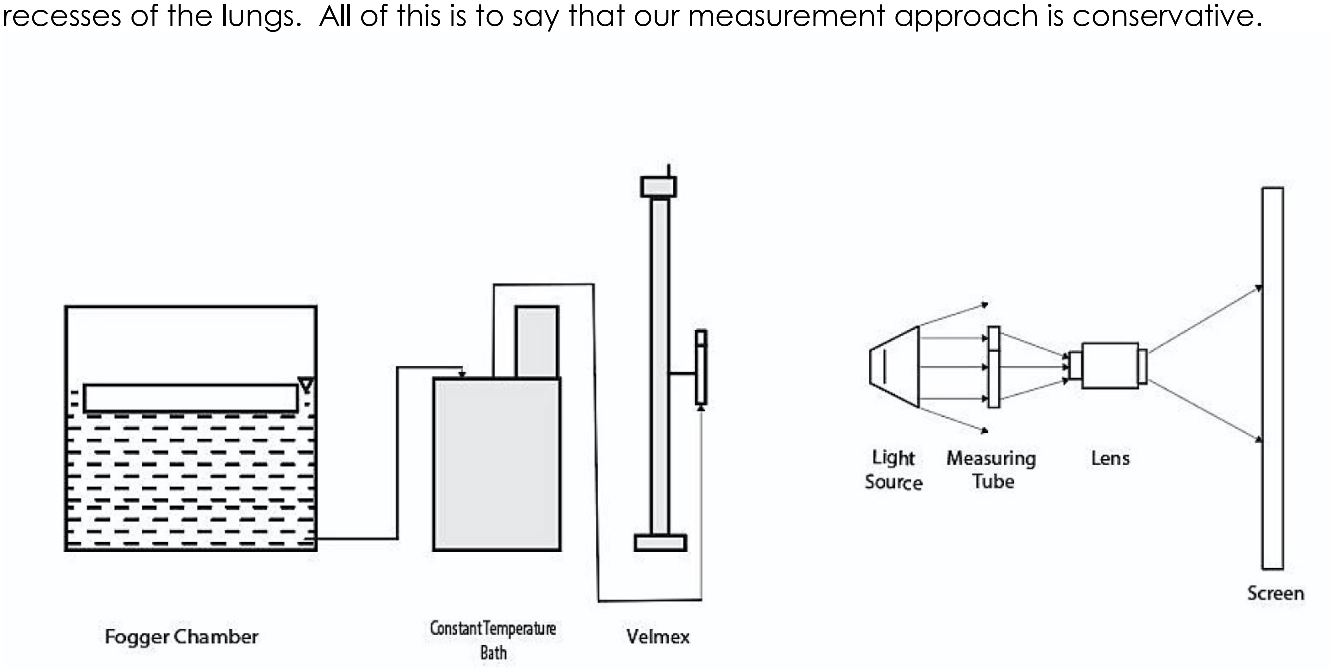

Figure 4 - Experimental setup used to quantify mass lost during the course of an experiment.

Experiments were conducted over a range of air flow rates Q and droplet number densities N_d. During each experiment, the setup was operated sequentially in a fog-off and a fog-on mode. Each mode was run for 10 minutes. For one experiment, each mode was run three times i.e. each experiment took 60 minutes and consisted of three fogger off on cycles.

In order to determine how the drop number concentration, N_d affects scavenging, it was necessary to obtain the rate of water consumption from the fogging chamber. This was then used to obtain N_d according to the equation:

$$N_d = \frac{\frac{6\dot{m}}{\rho \pi d_d^3}}{Q}$$

where $\dot{m}$ is the water mass consumption rate and d_d is the fog drop diameter. The challenge to this approach was computing the water consumption rate. This number was not large; the decrease in the water level over the course of an hour was on the order of millimeters and so any approach based on measuring the drop in water level using a ruler was precluded due to the presence of the meniscus at the tank wall; said meniscus being comparable to the drop in water level and exhibiting stick-slip behavior as it moves. Accordingly a more involved approach was necessitated and is shown in Figure 4, with a more detailed view presented in Figure 5. As these figures show, a tube was connected between the fogging chamber bottom and a graduated tube (basically a thin test tube with fine scale grating etched into its surface). In between the fogger and the graduated tube, the connecting tube passed through a circulating refrigerated water bath (RMG Lauda Brinkmann). This approach was needed to ensure that any bubbles in the water that might exist or form would be eliminated by cooling the water and forcing the gas into solution. This was done because the expansion/contraction of bubbles caused errors in earlier versions of this approach. The water bath was set to 15°C. A valve was located just before the water bath. The graduated tube was mounted on a unislide assembly (Velmex UniSlide A40 Series) which has a high precision lead screw and a graduated knob. A magnified image of the water level in the graduated tube was obtained as indicated in Figure 4 and Figure 5 using a 500-watt halogen light source, and a camera lens (Nikon, Micro Nikkor 105 mm) which projected the image onto a large frosted screen.

Before starting an experiment, the unislide assembly was adjusted so that the water level in the graduated tube was located at a predetermined location on the tube, which position was recorded. The valve was then closed, and the experiment was conducted. After the experiment, the valve was opened, causing the water level in the graduated cylinder to drop. Observing the magnified image of the new water level on the frosted screen, the unislide knob was rotated until the water level returned to its original position. The distance of travel of the unislide is equal to the drop in water level (it is noted that the volume of water in the graduated tube was negligible compared to the fogger tank volume), and this value was recorded. The volume of water consumed in the fogging chamber was then calculated by multiplying this vertical displacement by the internal footprint of the fogging chamber. The above equation was then used, with the fog size distribution of Merrell and Saylor (2017) invoked to account for d_d in that equation. Merrell and Saylor (2017) used the same fogger as in these experiments; the average diameter for that distribution was d_d = 5.8 um, close to the nominal diameter of 5 um quoted by the fogger manufacturer.

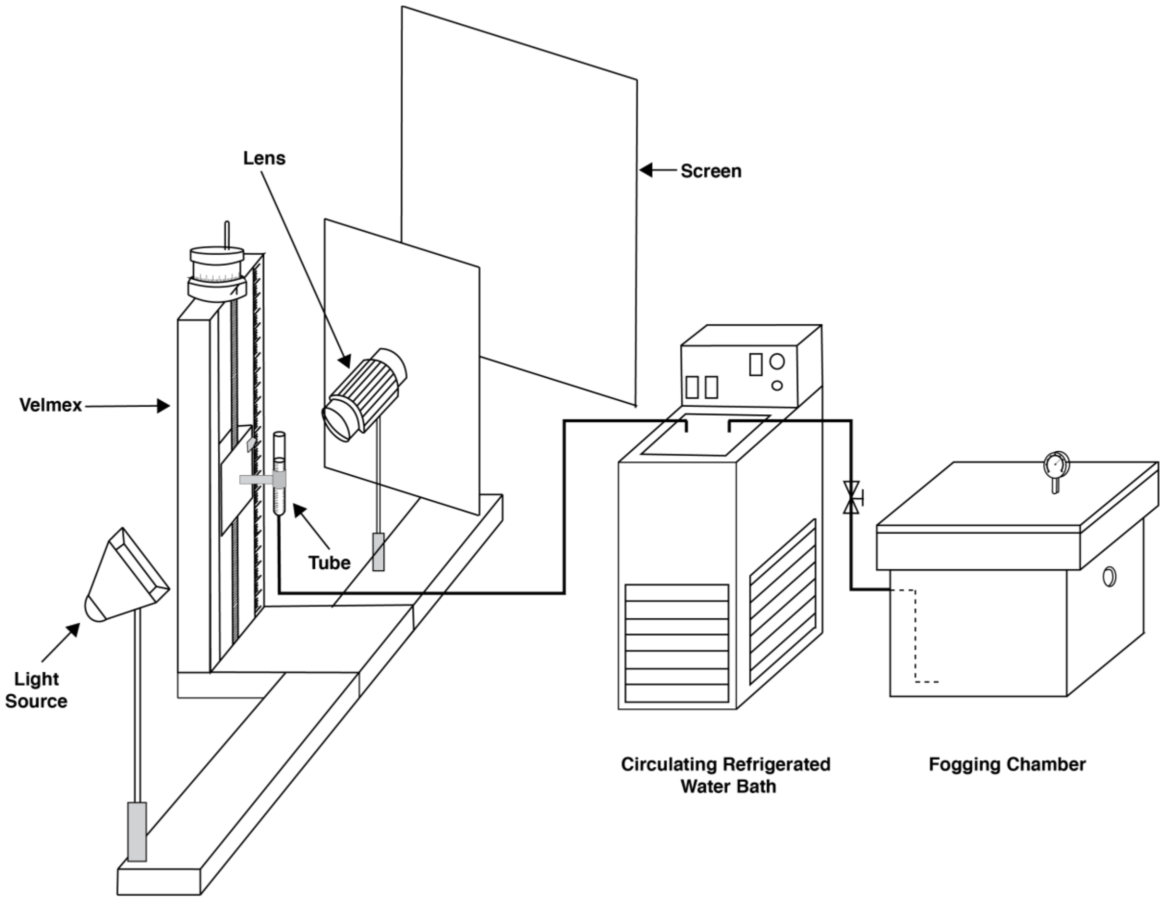

Figure 5 - Alternate view of the setup shown in Figure 4.

Overall, the above approach enabled measurement of particle number densities upstream and downstream of the fogging chamber using the two NanoScan units. These units provided these number densities over a range of particle diameters. Also measured were the drop number density and air flow rate. These measurements enabled computation of the particle scavenging coefficient and the particle agglomeration coefficient (as described below) and allowed these to correlated to the air flow rate, drop number density, and particle diameter, all of which are presented in the next section.

<u>Engine Test-Cell Experiments</u>

To ascertain the performance of the fog scrubber on actual diesel particulate matter (DPM), the setup used above was modified for use on a diesel engine and experiments similar to those described above were conducted. The setup shown in Figure 6 was used wherein DPM concentrations were taken upstream and downstream of the fogging chamber to ascertain the efficacy of fog on DPM removal. The primary components of the system consisted of a diesel engine, exhaust cutout, dynamometer, heat exchanger, fogging chamber, surface drain, cyclone separator, and measurement instrumentation as shown in Figure 6. Details of each component are now described.

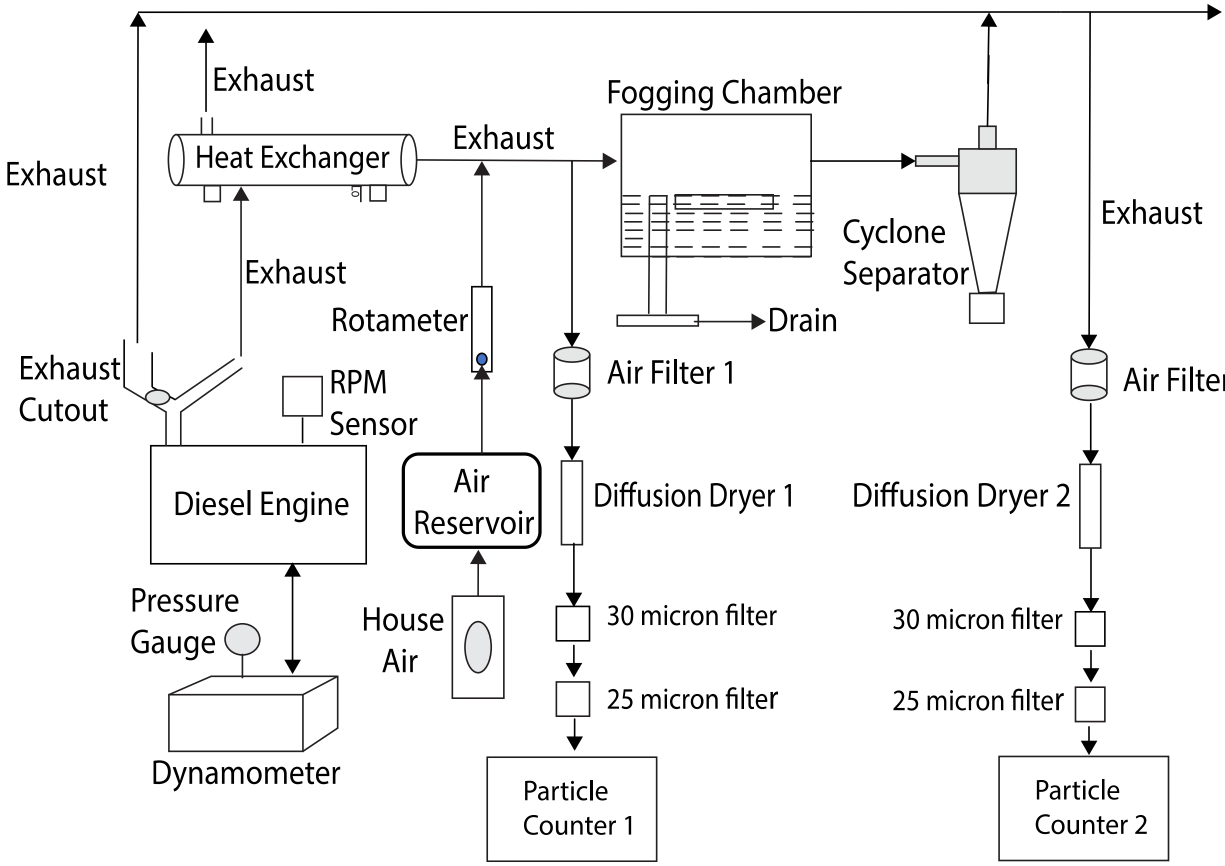

Figure 6 - Setup used to test DPM scavenging of diesel exhaust in the engine test-cell environment.

<u>Diesel Engine</u>

A Daihatsu DM700D diesel engine was the source of diesel exhaust for the system. The engine featured a displacement volume of 697cc and a maximum operating load of 13.2 kW. The degree of engine exhaust back pressure due to the heat exchange (see below) and fogging system was monitored by a pressure gauge and the exhaust manifold was coupled with an electric exhaust cutout valve to control this back pressure. The cut out valve was partially opened (around 20%) to limit the exhaust flow that enters into the heat exchanger (and hence the fog chamber). The hydraulic dynamometer was used to apply a torque load on the engine per stated test conditions (see Table *1*, below).

<u>Heat Exchanger</u>

The incoming diesel exhaust had a very high temperature (as high as 350 ºC) and needed to be cooled down below its saturation temperature to avoid evaporation of the water and fog drops inside the fogging chamber. A shell and tube heat exchanger (Armstrong, Model W6244) was used to cool down the exhaust to 19 ºC - 25 ºC. The water side of the heat exchanger was supplied by the tap. The heat exchanger was run in a once-through capacity and was very successful in cooling the exhaust. Future work in this area should focus on a closed-loop system where a radiator receives the water after the heat exchanger and rejects the absorbed heat to the environment. This is discussed in the Future Work section, below.

Fogging Chamber

The fogging chamber used in these experiments made of acrylic sheet and had a volume of 1000 in^3 (0.0163 m^3). It contained a 12 head ultrasonic foggers (The House of Hydro, Model DK12-36), floating at a height of 0.152 m beneath the water surface inside the fogging chamber. This fogger was a different, but identical fogger from the one used in the laboratory experiments described above. It has a power rating and an operating frequency of AC36V, 290W and 1.7±0.04 MHz, respectively. A significant challenge initially in this work was keeping the water surface clean. As exhaust flows over the water surface, films accumulate which are presumably diesel fuel, engine oil, and/or other hydrocarbon constituents of diesel exhaust. As this film accumulated, fog generation effectively ceased. To maintain continuous operation of the foggers, a surface drain system was integrated. This system removed the very top layer of the water surface, including accumulated films. This fluid was pumped through a filter using a small water pump and then returned back to the fogging chamber in a closed cycle. Downstream of the fogging chamber, the flow exited the system through the cyclone separator. The cyclone was designed for this application based on the Stairmand's prescribed optimum critical cyclone dimensions for high efficiency removal (Stairmand, 1951).

Measurement of the fog drop number density, N_d was much more challenging in the engine test cell environment than for the laboratory environment. The surface drain and the presence of vibrations made the approach taken in the laboratory experiments impractical. To obtain this measurement, a separate set of experiments was conducted where house air instead of diesel exhaust was flowed into the system with the fogger turned on. By running this air flow for several hours, a significant drop in the water level was recorded (the surface drain was not operated) and the mass flow rate computed. Data was acquired for a range of air flow rates. Since the maximum house air flow exceeded the engine exhaust flow rates explored here, the air data was extrapolated to the exhaust flow rate for each engine loading condition explored. Using an assumed drop diameter of 5 um, the drop number density for each operating condition was thereby obtained.

Particle Sampling with Dilution System

Under the conditions explored here, the number density of DPM exceeded the upper measurement bound of the NanoScan particle counters (the same units that were used in the laboratory experiments described above), which was 10^6/cc. Accordingly, a dilution system was introduced to keep the number density of the particles within the operating range of the particle counters. The exhaust flow was mixed with house air before entering into the fogging chamber to accommodate the operating range of the particle counters. The dilution air flow rate was held at 188 lpm for all experiments. As a result, the dilution ratio changed depending on the exhaust flow rate resulting from the corresponding load applied. Since the degree of dilution was identical for the upstream and downstream NanoScans, this introduced no error, as long as the upper bound of 10^6 particles/cc was not reached. A significant amount of time and test experiments were conducted to create and modify the dilution system to ensure that the above statement was true.

For both NanoScans, filters were placed upstream of the sampling ports to ensure that large, micron-scale particles were eliminated, thereby protecting the NanoScans. Specifically, the flow first went through a 5.08 cm diameter tube filled with clean furnace filter material (air filters used in home air conditioners). These filters served primarily to slow the rate of clogging of the subsequent filters. The furnace filter was followed by a 30 micron filter, and then a 25 micron filter. A diffusion dryer was also placed in line to ensure that fog drops were not counted by the NanoScans. As was the case for the laboratory tests, the air accumulator was placed in line after the house air inlet to buffer any fluctuations in hour air pressure.

Emission Test Conditions

Experiments were conducted under three different loading conditions. The diesel engine shaft speed and the corresponding load are listed in Table 1. In each test, particles were sampled for five minutes without fog and then for five minutes with fog for a total of thirty minutes for each run.

Test Conditions.	Speed (rpm)	Load (hp)	Load (kW)
1	1,496	2.5	1.8
2	1,730	3.5	2.6
3	1,864	4	3.3

Table 1 - Speed and load for the runs conducted in the engine test cell environment.

The collected data was then analyzed to measure the scavenging coefficient and agglomeration coefficient both without and with fog.

4.0 Research Findings and Accomplishments: The highlight of the report should be a detailed documentation and discussion of the research findings and accomplishments. The presentation of this material should be organized in a manner that clearly relates to the specific aims and research objectives for the project. Data and information developed from the project efforts should be presented with sufficient detail, analysis, and interpretation to support a clear and full understanding of the research conclusions derived from the project.

In this section, results and conclusions obtained from the laboratory experiments and engine test-cell experiments are presented. For both sets of experiments, particle scavenging is characterized by two variables, the scavenging coefficient, E, and the agglomeration coefficient K. Both of these variables quantify the number of particles removed, but in different ways. The definition of E is:

$$E = \left(\frac{N_1 - N_2}{N_1}\right)$$

where N_1 and N_2 are the upstream and downstream number densities (particles/cc or particles/m^3), respectively, and where upstream and downstream refer to positions relative to the fogging chamber. The agglomeration coefficient is defined by the first order differential equation:

$$K = -\frac{1}{N^2}\frac{dN}{dt}$$

the solution of which is:

$$N\,(t) = \frac{N_0}{1 + N_0 K t}$$

From this equation, K is obtained by setting N_0 to N_1, setting N(t) to N_2, and by setting t to the residence time in the system. In this way, N(t) is N_2. It is noted that K and E are related by the equation:

$$K = \frac{E}{N_2 t}$$

Results for both E and K are reported below as a function of volumetric air flow rate, Q, particle diameter d_p, and droplet number density N_d. The two parameters, E and K, each provide different insight into the scavenging behavior. E provides a more intuitive feel for the scavenging process as it is simply the percent of the incoming particles that are removed. This enables a very clear ability to contrast the impact of fog for the situation at hand. However, E is sensitive to numerous parameters that don't necessarily illuminate the efficacy of fog. These include the residence time, and, importantly, the incoming particle number concentration. When the incoming particle concentration is high, E will be high, and when the incoming particle concentration is low, E will be low (everything else held constant). Hence, for a given particle removal strategy, one could, essentially, manipulate the situation to get almost any value of E, simply by increasing or decreasing the incoming particle number density. This is not necessarily a problem if the operating conditions of a system are very stable, in which case comparison of fog and no-fog conditions can be made. However, as is the case in the engine test-cell environment, where conditions vary and are difficult to control, fog/no-fog comparisons are challenging. The coagulation coefficient K does not suffer from this drawback. Indeed, if the geometric and flow factors are unchanged, K should be independent of the inlet number density of particles. It also does not vary with residence time (nominally). K does vary with the other facets of the system which control the efficacy of particle removal. For example, as we will see, K varies with the drop number density.

Laboratory Environment Experimental Results

Figure 7 is a plot of E versus Q for the laboratory experiments, where Q is the air volumetric flow rate in liters per minute (LPM). Here, E is computed for the total number of particles in the flow (particles of all diameters that the NanoScan is sensitive to), and results are presented with the fogger on and with the fogger off. In this and subsequent plots, the fog-on condition is denoted by a blue symbol and the fog-off condition by an orange symbol, and the vertical error bars corrrespond to 95% confidence intervals. In the following plots, two fogger conditions are identified, high "H", and low, "L". These are a compilatyion of experiments which resulted in high and low fog number density, respectively. "H" and "L" corresponded to an average fog number density of $N_d = 0.43 \times 10^{12}/m^3$, and $N_d = 2.63 \times 10^{12}/m^3$, respectively. Of course N_d is an important parameter in and of itself, and subsequent plots will show the behavior of E and K with respect to N_d in finer detail than just the high and low concentration results presented here.

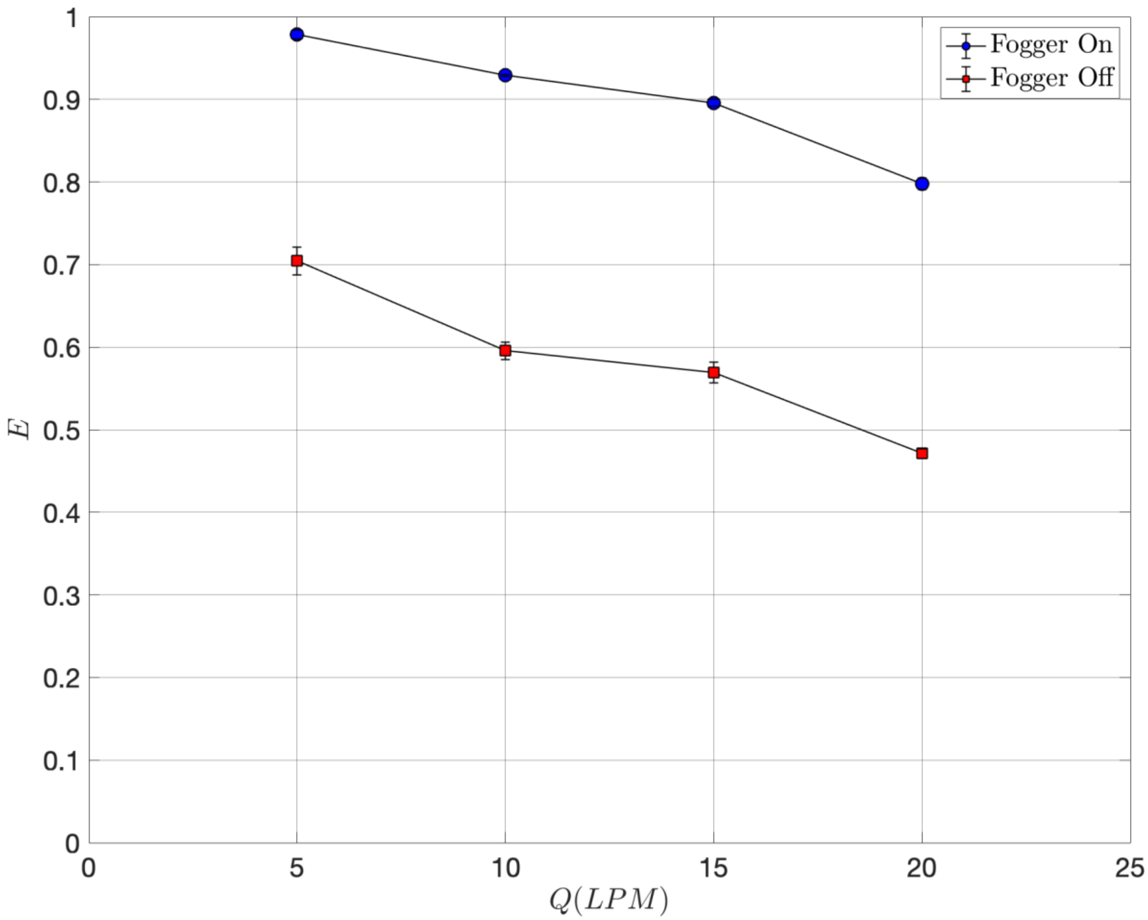

Figure 7 - Plot of E versus Q for the "H" fogger condition. The vertical bars are 95% confidence intervals. Note that for some runs these intervals are very small and therefore are obscured by the data symbol itself.

Figure 7 shows two important trends. First, that for both fog-on and fog-off conditions, E decreases with increasing volumetric flow rate, and second, the presence of fog has a significant impact on particle removal for these conditions. The former observation is expected; as the volumeteric flow rate increases, the residence time of particles in the overall setup decreases. Since, with or without fog, the processes which remove particles take time; a lower residence time allows less time for particle removal and hence E should decrease linearly with Q, a result which the data rougly show. For all four of the air flow rates explored here (5, 10, 15, and 20 LPM), the presence of fog significantly increased the scavenging coefficient. As the figure shows, this increase is approximately 0.3 on a range from 0 to 1.0 for all four flow rates. Of note, at 5 LPM, E increased from 0.7 to just less than 1.0, where 1.0

denotes complete removal of particles. Hence, the air exiting the system was almost perfectly clean.

Figure 8 presents the same results as presented in the E versus Q plot of Figure 7, but on K versus Q coordinates. Variations in upstream particle number density from run-to-run and the change in residence time due to different values of Q should not have an impact on K. The figure shows that K is roughly constant for the fog-on case, showing no real trend with Q. It is also significantly larger for the fog-on case than for the fog-off case, as expected. Indeed, at low Q, K is well over an order of magnitude larger for the fog-on case when compared to the fog-off case. At the maximum Q, K is a factor of 3 larger for the fog-on case. Interesting, there is a significant variation in K with Q for the fog-off case. Since this cannot be due to a residence time effect or a particle number density effect it is likely due to increased wall deposition due to the increasing velocity of the flow. This is possible, since the Reynolds number is transitional in these flows and at the higher flowrates, a burgeoning turbulence may increase particle deposition, as well as enhance secondary flows that may exist in the turns of the coil. It may be these effects that cause K to increase with Q in this plot.

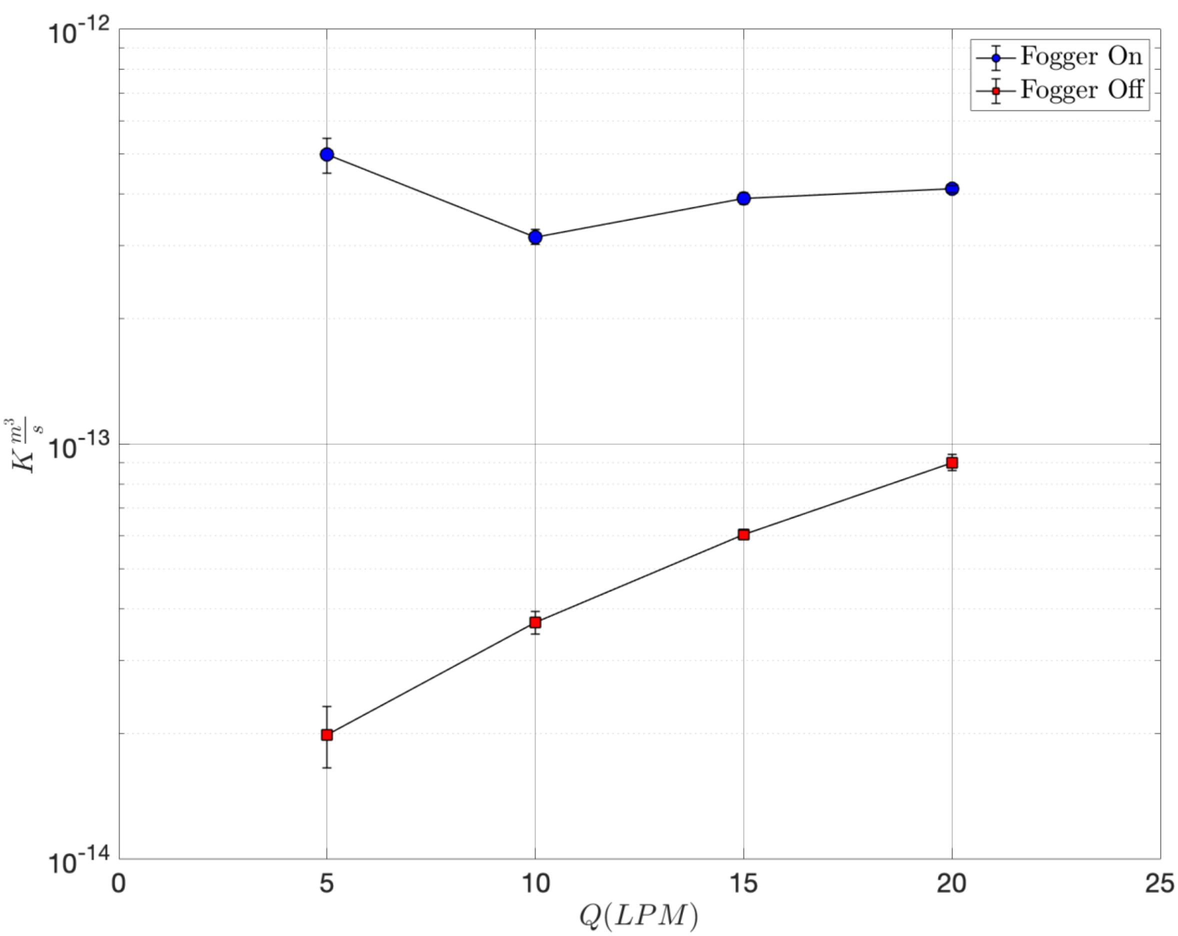

Figure 8 - Plot of K versus volumetric flow rate, Q for the "H" fogger condition. The vertical bars are 95% confidence intervals. Note that for some runs these intervals are very small and therefore are obscured by the data symbol itself.

Figure 9 is a plot of E versus d_p for a volumetric flow rate of 15 LPM. This plot shows, in essence, that as the particle diameter gets bigger, the scavenging coefficient gets smaller. This is true for both the fog-on and fog-off cases. This is expected, since the diffusivity of particles decreases with increasing d_p. This diffusivity enhances scavenging in the no-fog case, enabling particles to diffuse toward the wall. It also enhances scavenging in the fog-on case in that the particles are better able to diffuse to the drops. At the two smallest particle diameter bins (11.5nm and 15.5nm), the data do not support the above mechanism. Between these two points, E increases a bit with particle diameter, and the no-fog case actually exceeds the fog case (at least this is true at 11.5nm; for 15.5nm, E is essentially the same for fog-on and fog-off conditions). It is noted that, though small, the 95% confidence interval in the smallest diameter bin is larger than the other bins. Also, at these diameters, particle-particle agglomeration is going to be most significant. Hence, it may be the case that particles too small to be sensed are combining to form 11.5 nm particles, resulting in a *perceived* creation of particles, and decreasing E from the value it would otherwise have attained, and also reducing the reproducibility of the results for this bin (increasing the 95% confidence interval). Overall, this plot shows that, again, the presence of fog has a significant impact on scavenging. For the largest bin, the improvement in E is from 0.3 to 0.8 on a scale from 0 to 1.0, a 50% inrease.

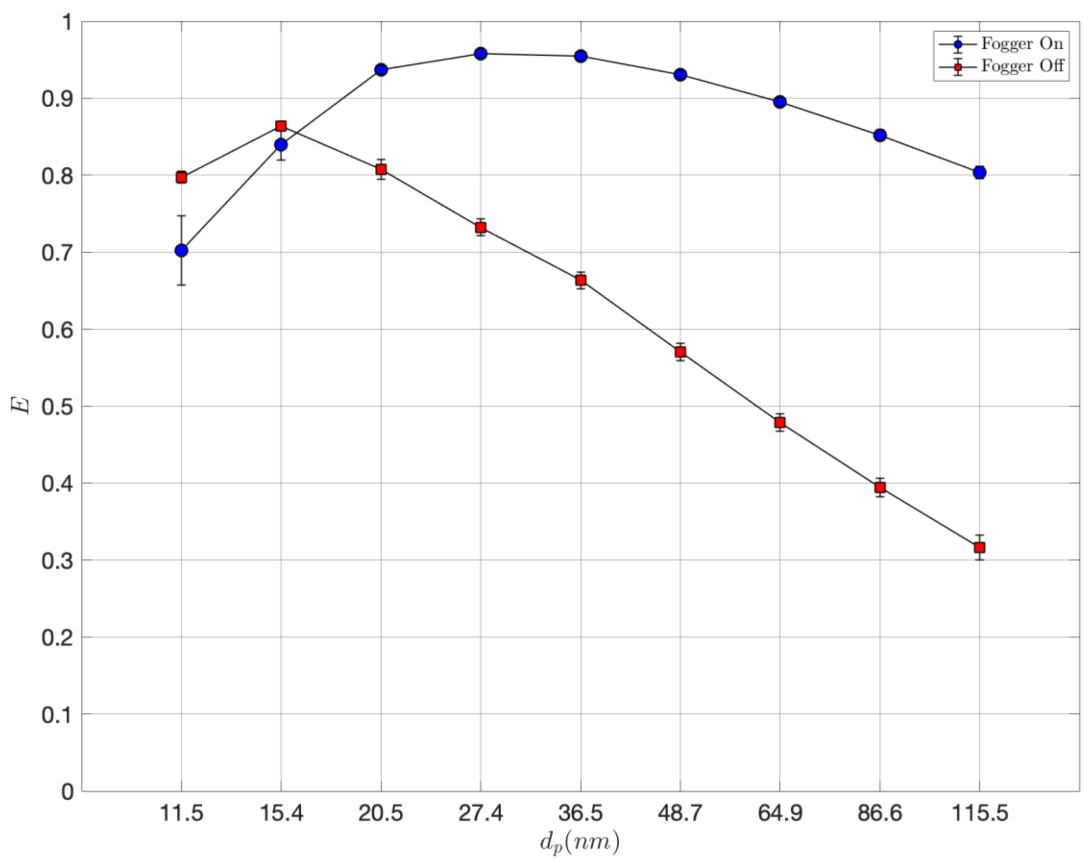

Figure 9 - Plot of E versus particle diameter, d_p in the laboratory test environment for both the fog-on and fog-off case at a volumetric flow rate for air of Q = 15 LPM. . The vertical bars are 95%

confidence intervals. Note that for some runs these intervals are very small and therefore are obscured by the data symbol itself.

Figure 10 presents the same data as in Figure 9, presented on K versus d_p coordinates. The improvement in K due to fog is, again, robust, slightly less than an order of magnitude at a particle diameter of 27.4 nm and somewhat smaller at other diameters. The anomalies at 11.4nm and 15.4 nm are observed here as well.

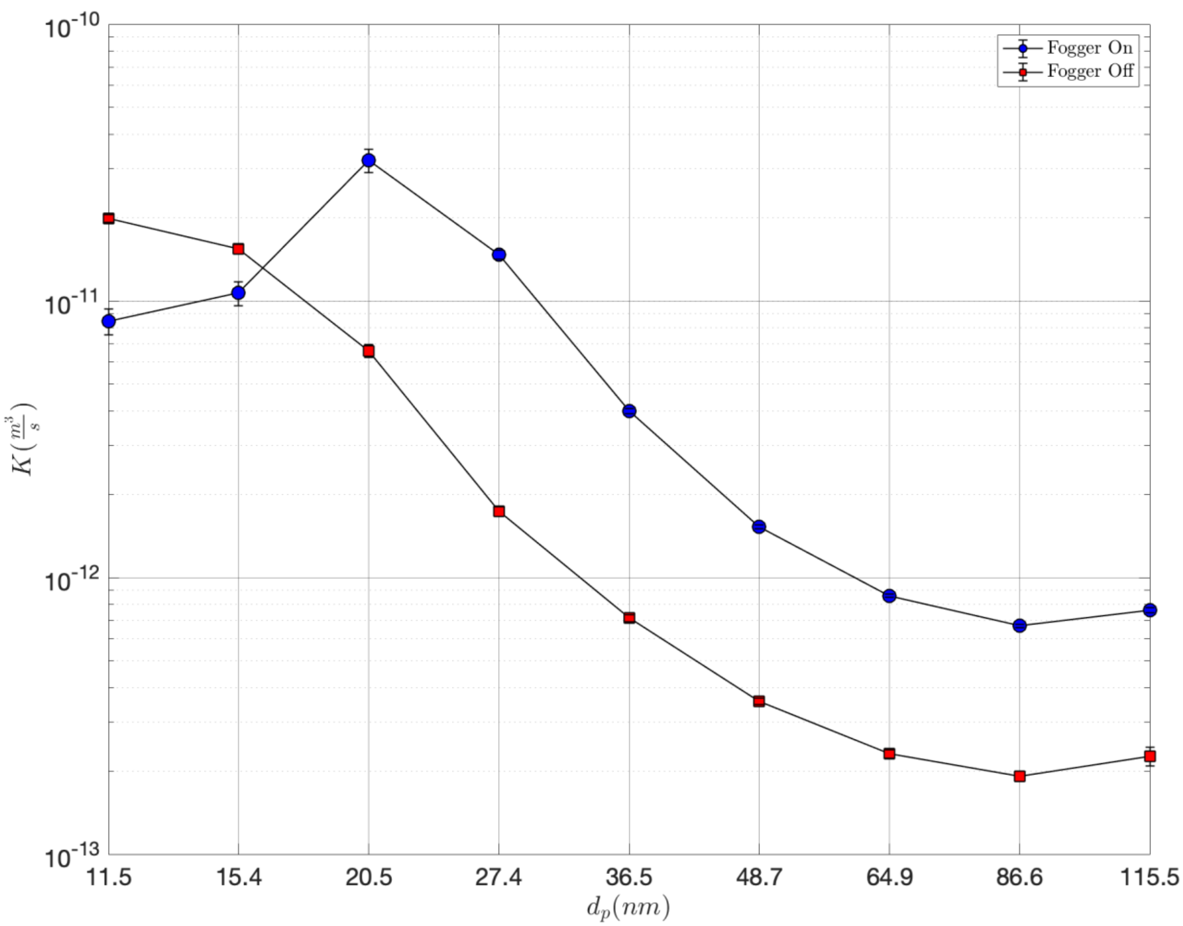

Figure 10 - Plot of K versus d_p at a volumetric flow rate of Q = 15 LPM. This plot is for the same data as presented in Figure 9. The vertical bars are 95% confidence intervals. Note that for some runs these intervals are very small and therefore are obscured by the data symbol itself.

To show the effect of drop number density, E is plotted against N_d in Figure 11 and K is plotted against N_d in Figure 12. We note that for a given power applied to the fogger assembly used in the laboratory setup, the values of N_d would fluctuate; higher power yielded larger N_d, but the reproducibility was poor. This was why such pains were taken to measure the water consumption rate, thereby enabling measurement of N_d, as described earlier in this report. It was these measurements that enabled accurate knowledge of the values of N_d presented in Figure 11 and Figure 12, below. Hence, though the drop number density varied from run-to-run under nominally identical conditions, this is not a concern since the value of drop number density was accurately measured. The plot of E versus N_d in Figure 11 shows an increase with N_d as expected, but not a very large increase. This is likely due to the simple fact that under these conditions, E is quite high, which is to say, most of the particle have been scavenged by the time the flow exits the setup, and further improvements are difficult to attain. The plot of K versus N_d shown in Figure 12 does not suffer from this issue, since the effect of particle number density is not present. And, this figure shows a noisy, but nevertheless significant increase in K with N_d. Indeed, K increases by about one order of magnitude as N_d increases by a factor of 5.

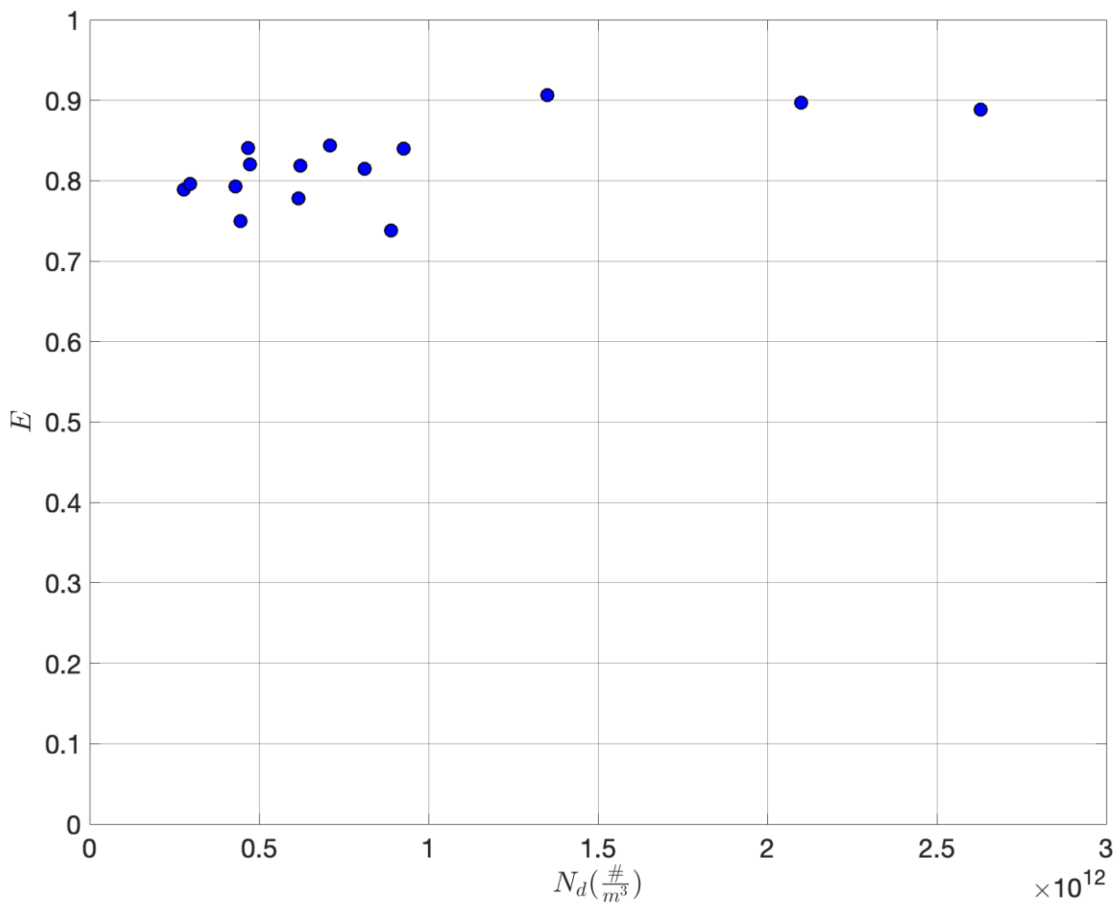

Figure 11- Plot of E versus fog drop number density, N_d at an air volumetric flow rate of Q=15 LPM.

Though noisy, Figure 12 is perhaps the most significant result of the laboratory test experiments. The prior plots show the expected results that scavenging decreases with particle diameter. Also, the prior plots show that E itself increases with residence time. Both of these are important and can be used in future designs of fog scrubber systems. But Figure 12 indicates that it is the drop number density which enables an increase in K, the one variable that can be controlled in an actual implementation. Stated another way, the particle diameters and the volumetric flow rates of an engine are not subject to change. However, the amount of fog drops introduced in a scrubber can be controlled, and this plot shows significant increase in K as that number density is increased.

It is noted that the flow rates employed in the laboratory experiments are very low by engine standards. For example, a 5 liter engine operating at 2000 rpm (modeled as a simple air pump), would yield an exhaust flow rate of approximately 10,000 lpm, 500 times as large as the maximum flowrate explored in the laboratory experiments presented above. However, if we imagine traveling with the flow, it is not the speed of the flow that impacts K (ignoring potential improvements in scavenging due to turbulence), but rather the ability of a particle to diffuse to a drop. This will occur as long as the particle-to-drop distance is relatively small. Stated another way, as long as the drop number densities attained in the laboratory can be replicated in an engine environment, the excellent scavenging performance seen in the laboratory should also be seen in the engine. Figure 12 shows that this number density should be on the order of 10^{12} drops/m^3 (10^6 drops/cc).

Of course turbulence will grow in intensity with increasing flow rate, but this will only serve to further enhance scavenging, increasing values of both E and K.

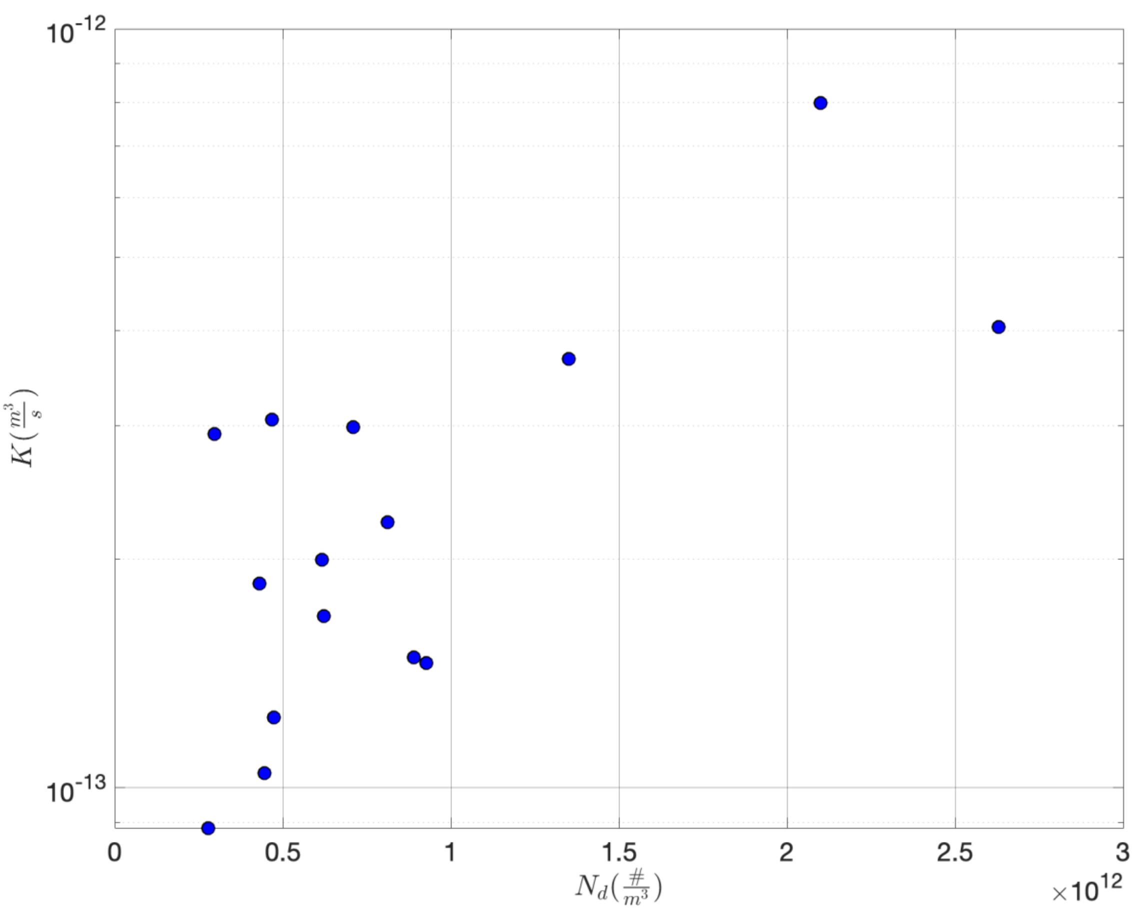

Figure 12 - Plot of K versus fog drop number density, N_d for air volumetric flow rate Q=15 LPM. This data is the same as that presented in Figure 11.

Engine Test-Cell Experimental Results

The test conditions evaluated in the engine test-cell environment are presented in Table 2 showing the load placed on the engine, the flow rate through the fogger, and the drop number density.

Test Conditions.	Load (hp)	Load (kW)	Exhaust Flow Rate (lpm)	Drop Number Density (/m^3)
1	2.5	1.8	521	1.13×10^{12}
2	3.5	2.6	600	1.07×10^{12}
3	4	3.3	636	1.05×10^{12}

Table 2 – Engine load, exhaust flow rate and fog drop number density for engine test-cell experiments.

As expected, the ability to control the operating conditions in the engine environment was significantly lower than for the laboratory scavenging tests. Among factors that were difficult to control include: variations in particle number density, even at constant engine load and rpm, contamination of the water surface due to deposition of hydrocarbon films on that surface, in spite of the presence of the surface drain, and deposition of subsequent release of deposited diesel on the internal walls of the apparatus. A consequence of this is that the time traces of the particle number density, time traces of E, and time traces of K were all variable. As one example of this, Figure 13 shows a time trace of DPM particle number density (total) for both the upstream and downstream NanoScan particle counters, with fog-off/fog-on periods indicated. The time trace shows firstly a roughly continuous increase in particle number density for both upstream and downstream particle counters (note that the y-axis is logarithmic). This variation in number density with time is not atypical and is not alleviated by simply letting the engine run for longer periods of time in the hope of achieving a steady-state. This type of variation seems to simply be inherent in this type of low-cost engine (and likely any engine lacking a closed-feedback control system of some kind).

An important goal was, of course, to determine the effect of fog on scavenging of actual DPM, and variations like those in Figure 13 can obscure the effect of fog. Since E tends to increase with overall particle number density, should a rise in number density occur after a fog-on to fog-off transition, this can actually result in a higher value of E for fog-off than for fog-on. Moreover, occasionally, clearly spurious points can occur. An example of this can be seen at minute 2 in the time trace. Experience with the setup suggests that this may be due to particles coming off of the tube walls in the setup. This is evidenced by the fact that more reproducible results are attained after the setup is cleaned. Nevertheless, events like those in minute 2 are not uncommon.

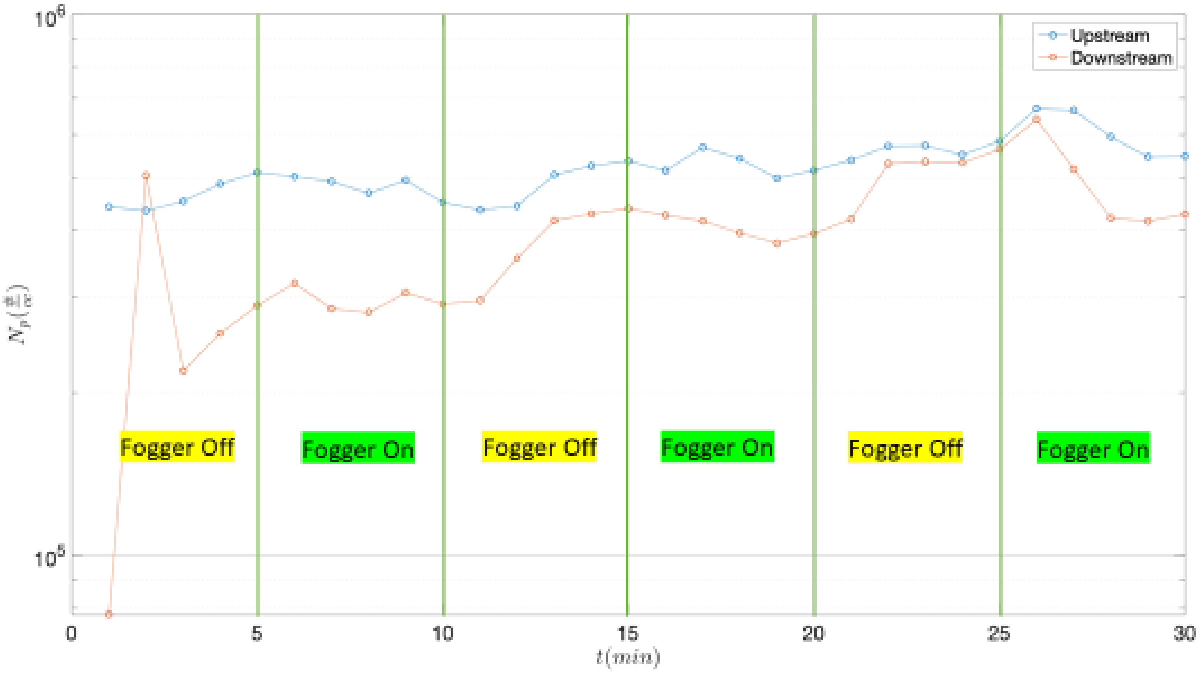

Figure 13 - Time trace of N_p (all diameters) for the engine test cell setup showing the upstream and downstream values. Intervals with fog on and fog off are indicated. Note that the N_d measurements lag the change in fogger conditions by two minutes. As noted in the text, this is the time delay due to the residence time in the sampling lines leading from the experiment to the NanoScans.

The impact of the above effects are further revealed in Figure 14 which presents the time trace for E for the data presented in Figure 13. First, the event at minute 2 results in a drop in E to a negative value. Also, though for most of the intervals it is clear that E is greater for fog-on than for fog-off, there is an overall decreasing trend in E, regardless of whether the fog is on or off (note that there is a 2 minute delay in the impact of turning the fog on and off due to the delay transport of the sample from the sample taps to the NanoScans). This has the consequence that, for example, even though E is smaller for the fog-off condition of minute 10-15 than for the fog-on condition from minute 15-20, it is also true that the fog-off condition of minute 10-15 is comparable to the fog-on condition of minute 25-30. When time traces like these are condensed to provide overall trends of E versus, for example, Q, the effects of fog are blurred out and significant uncertainty in the form of large 95% confidence intervals results.

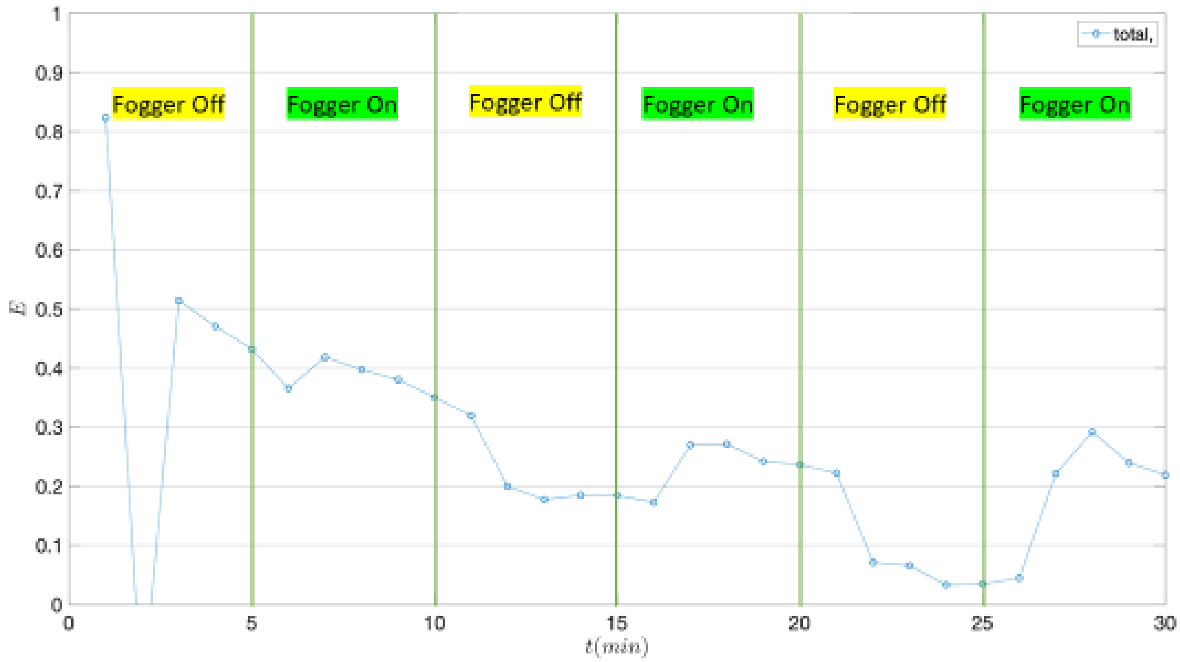

Figure 14 - Time trace of E computed for the data presented in Figure 13.

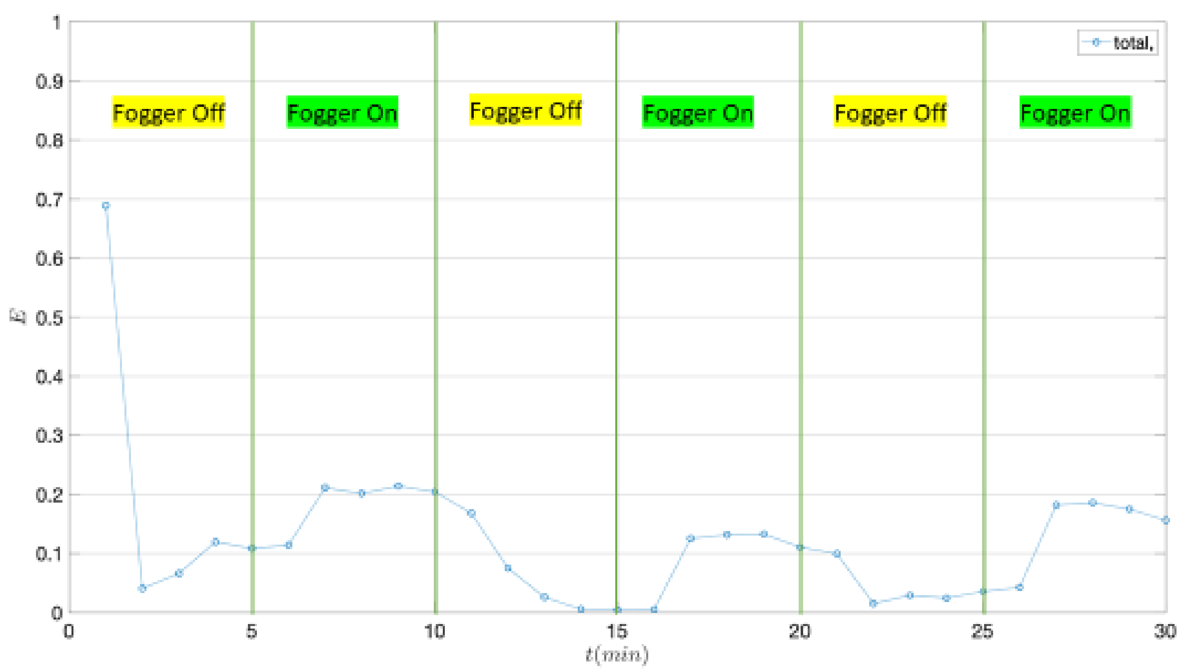

Figure 15 - Time trace for E in the engine test cell environment showing more stable conditions than in Figure 13 and Figure 14.

Of course, there were runs when the behavior of the system was much more stable (as well as those where the behavior was worse). For example, Figure 15 shows a time trace for E where the values for both the fog-on and fog-off are stable and there is only one spurious point. All of the above notwithstanding, the positive impact of the fog scrubber on DPM removal can be seen. However, the results do contain significant variability and correspondingly large 95% confidence intervals, as is now shown.

A compilation of the DPM results are now presented. Figure 16 – Figure 18 are plots of E versus d_p for fog-on and fog-off conditions for engine loads of 2.5hp, 3.5hp, and 4hp, respectively. The results show an increase in E due to fog for all diameters plotted and for all engine loads. It is noted that the 95% confidence intervals span these differences, however, it is strongly suspected that this is due to the issues described above and that further work in an environment where the engine can be better controlled would reduce these confidence intervals and increase the difference between the fog-on and fog-off averages. It is noted that for some of the diameter bins, E was negative. As this is physically impossible, it is also attributed to spurious data like that discussed above. A plot of E versus engine load is presented in Figure 19 where E is computed using the total particle number density (particles for all diameters). All of these plots (Figure 16 – Figure 19) show, independent of particle diameter and engine load, an increase in scavenging in the presence of fog of about 5%. Again it is expected that this difference would be larger in a more stable engine environment.

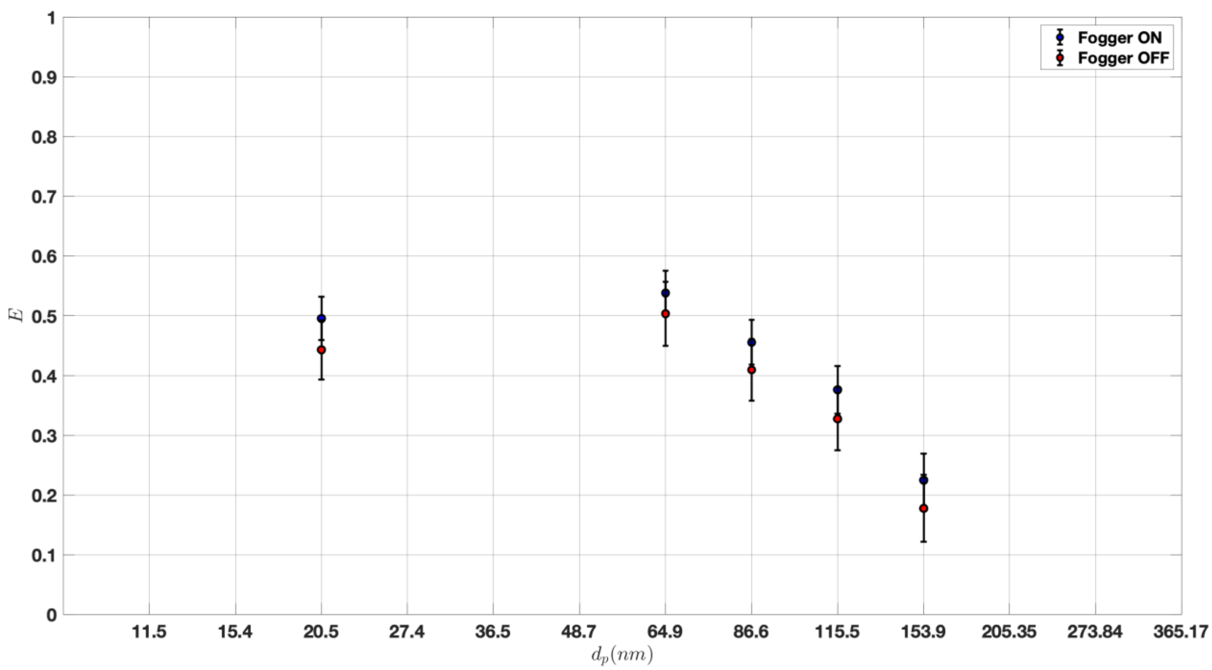

Figure 16 - Plot of E versus DPM particle diameter d_p including the fog-on and fog-off conditions at a loading of 2.5 hp.

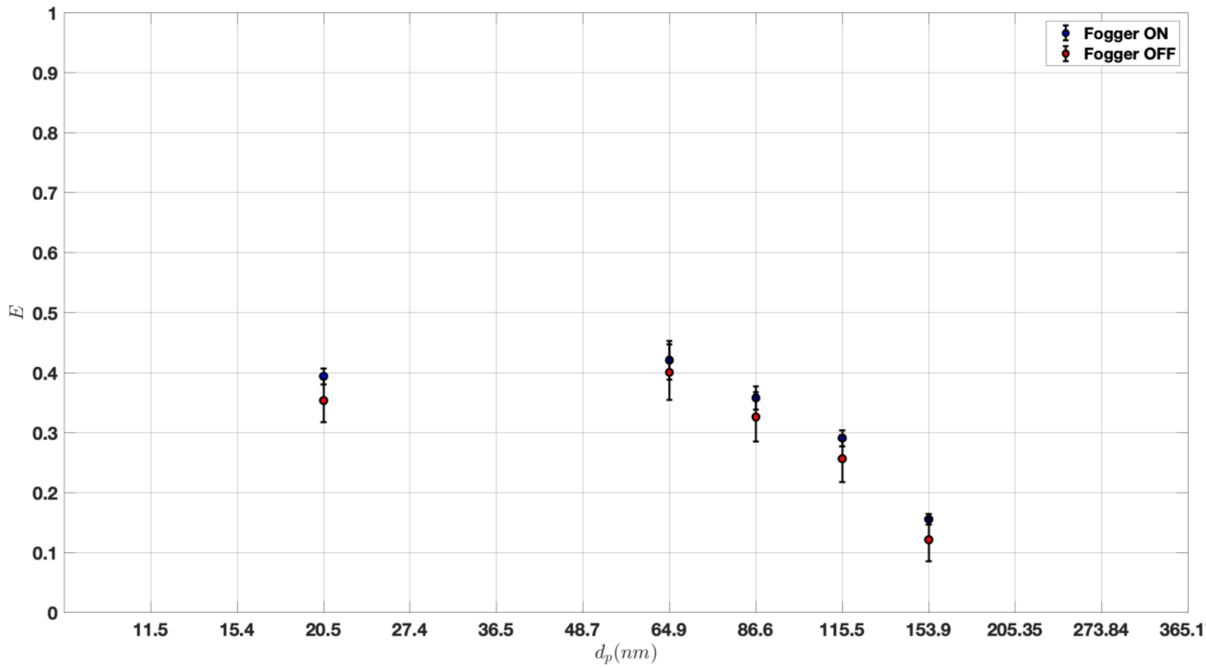

Figure 17 - Plot of E versus DPM particle diameter d_p including the fog-on and fog-off conditions at a loading of 3.5 hp.

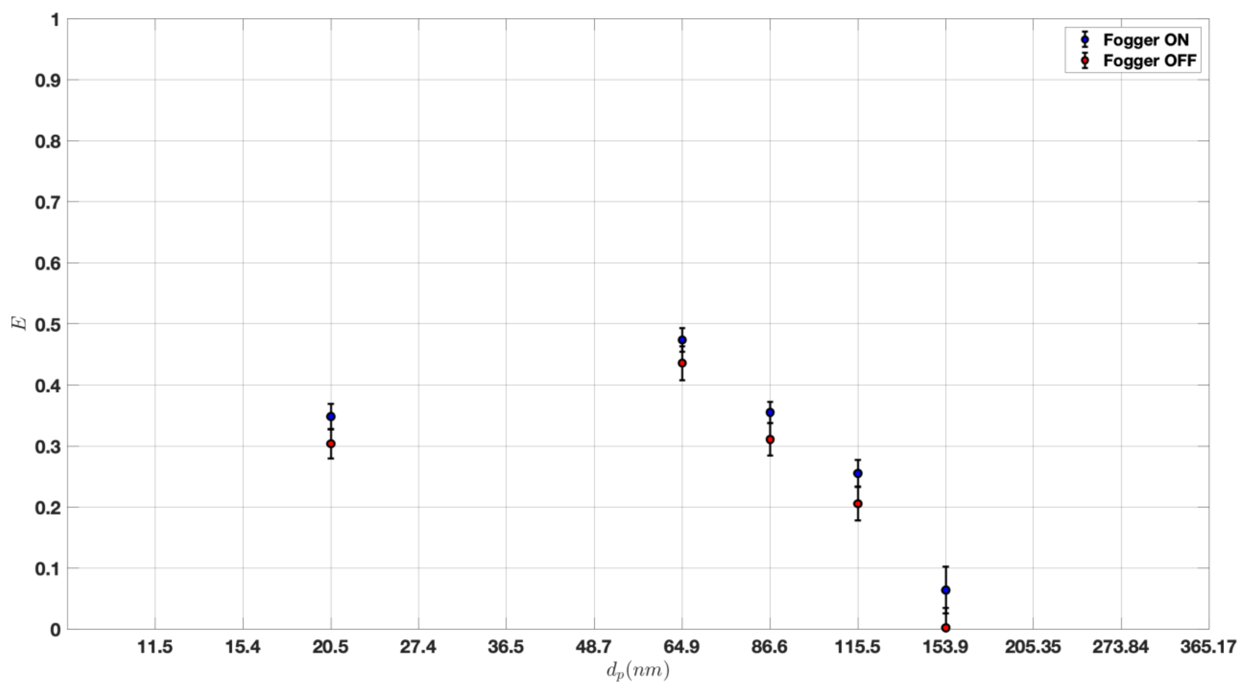

Figure 18 - Plot of E versus DPM particle diameter d_p including the fog-on and fog-off conditions at a loading of 4.0 hp.

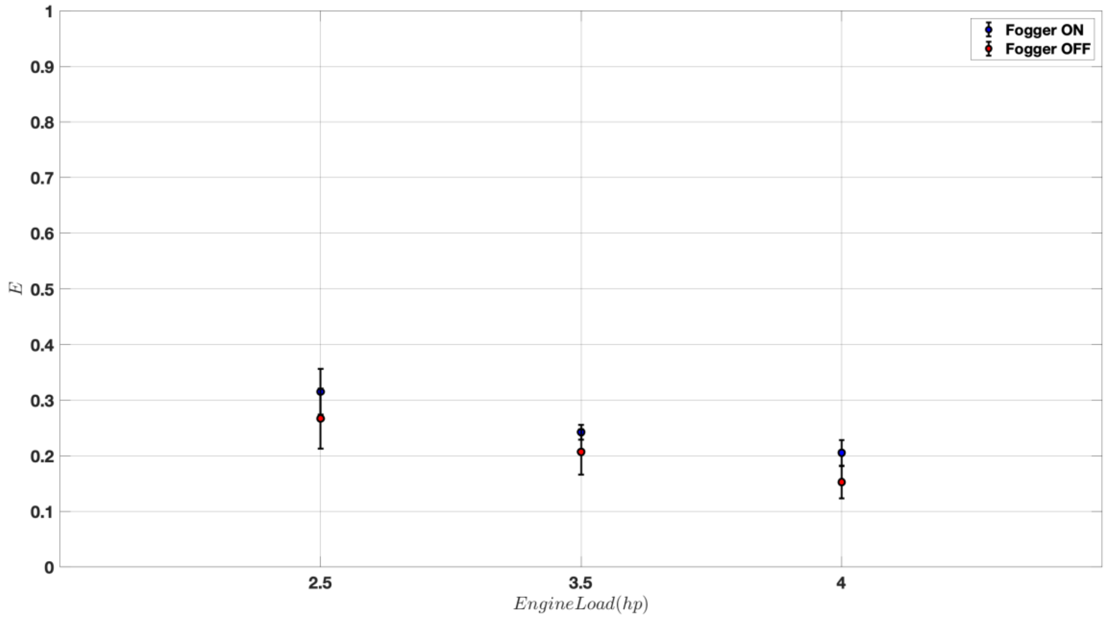

Figure 19 - Plot of E versus engine load for DPM particles of all diameters for fog-on and fog-off conditions.

Figure 20 - Figure 23 are analogous to the four previous plots with K as the y-axis. Again, the 95% confidence intervals are large precluding a confident statement of the improvement in K with fog. However, every plot shows an increase in K with fog for all conditions and all size bins. Figure 23 shows an increase in K due to fog of 25% at 2.5hp engine loading, an increase of ~20% at 3.5 hp and an increase of ~15% at 4hp.

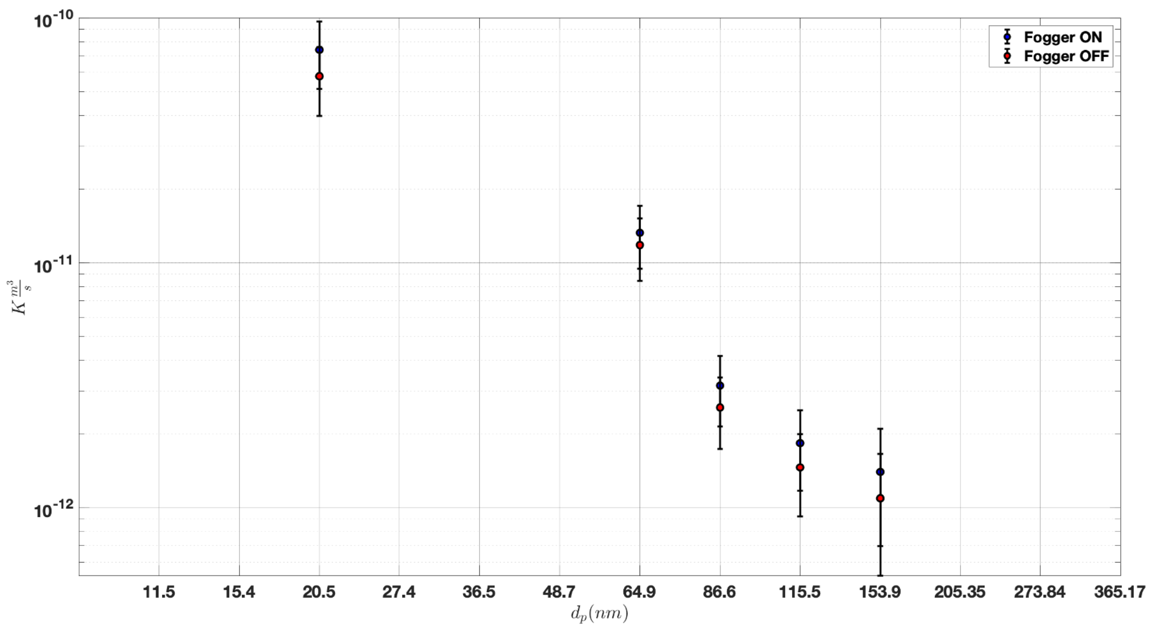

Figure 20 - Plot of K versus DPM particle diameter d_p including the fog-on and fog-off conditions at a loading of 2.5 hp.

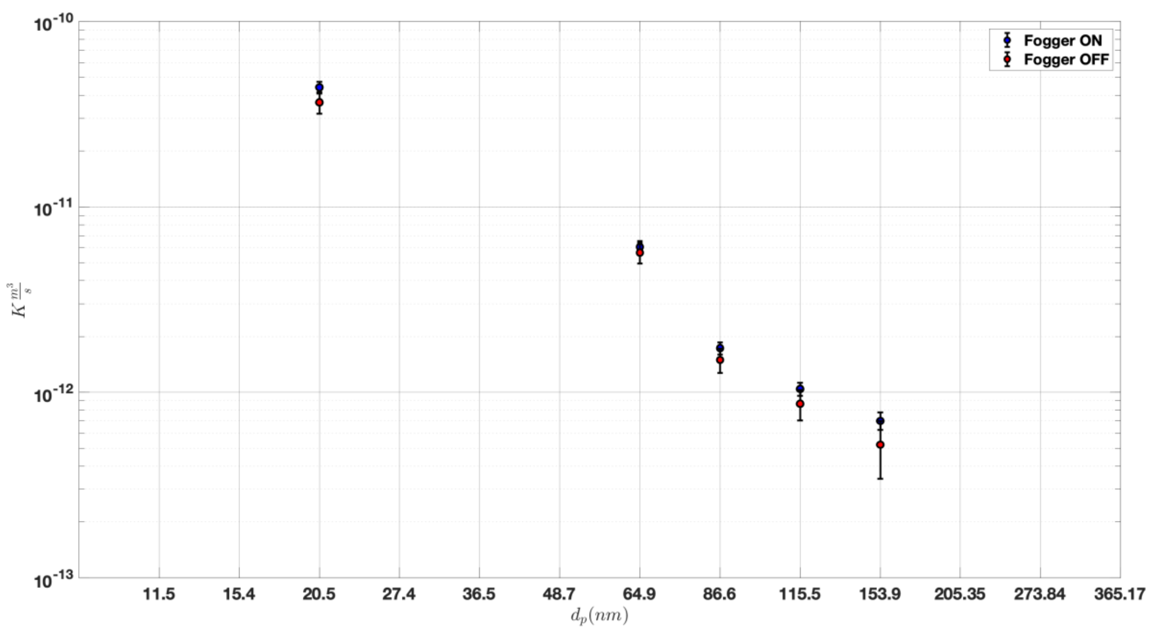

Figure 21 - Plot of K versus DPM particle diameter d_p including the fog-on and fog-off conditions at a loading of 3.5 hp.

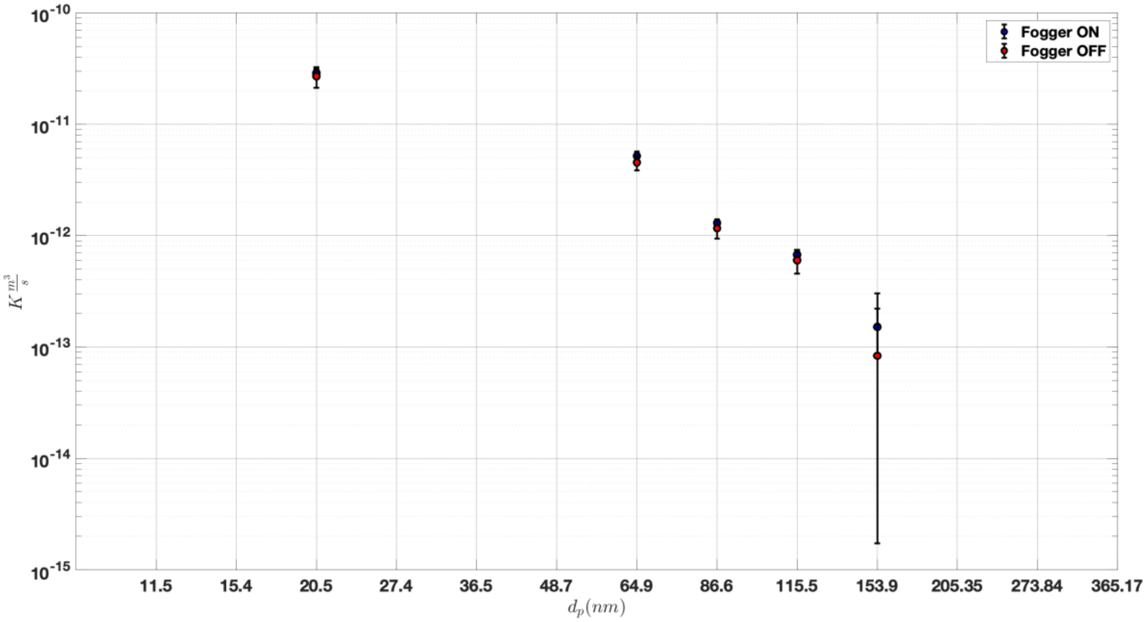

Figure 22 - Plot of K versus DPM particle diameter d_p including the fog-on and fog-off conditions at a loading of 4.0 hp.

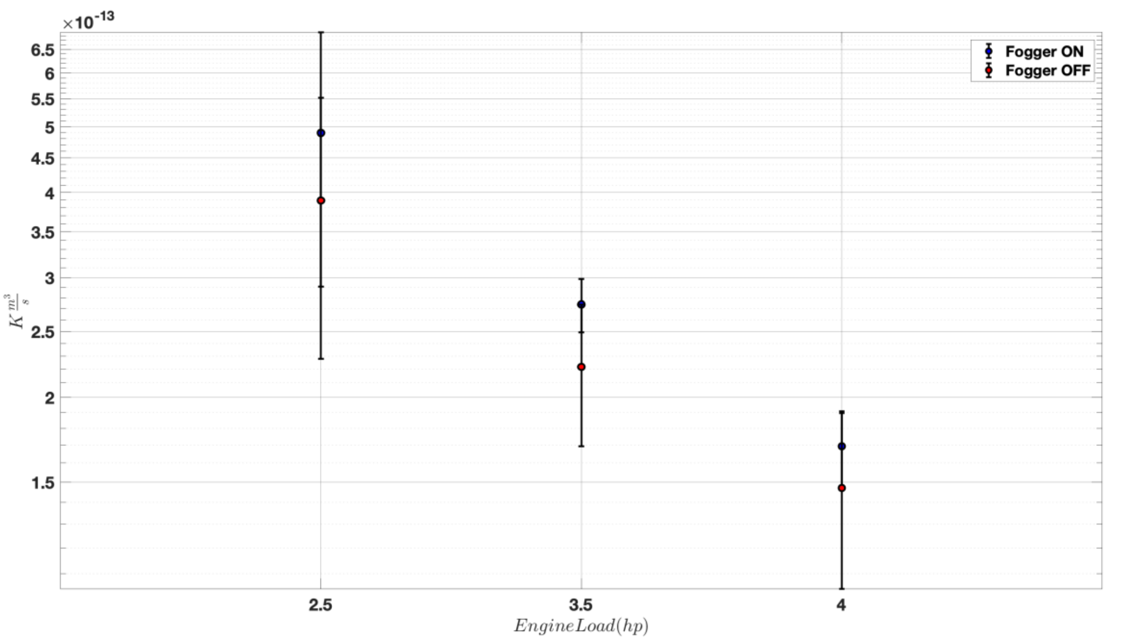

Figure 23 - Plot of K versus engine load for DPM particles of all diameters, showing effect of fog-on versus fog-off conditions.

To quantify the overall improvement in scavenging using fog for these DPM runs, the fractional improvement in E was computed and is plotted in Figure 24. Again, the 95% confidence intervals are large, but these show that the overall improvement ranges from 5% to 15%.

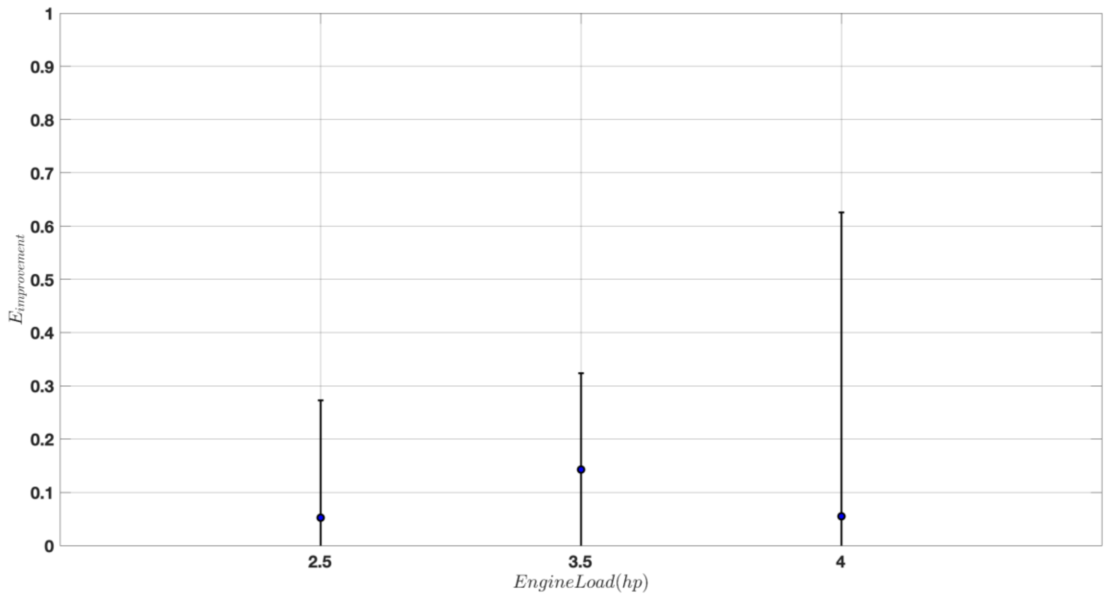

Figure 24 - Plot of improvement in E due to fog versus engine load.

Further work would be required to make these experimental diesel engine more repeatable. It is the opinion of the PI's that, given the fact that the droplet number density (as well as the method for creating drops) shown in Table 2 presented above, is the same in the engine and laboratory environments, that it is likely that the percent improvement due to fog in these engine tests is probably comparable to the laboratory environment, and that the decrease in performance observed going from the lab to the engine is simply due to an inherent variability in the operating environment that blurs the results.

5.0 Publication Record and Dissemination Efforts: In addition to summarizing the accomplishments, a complete record of presentation, publications (including those in process) and deliverables shall be provided. (Note: Only a (bibliography) listing of the reports is required. Do not provide copies of the publications.) In addition to this record, a dissemination plan shall be provided for any enabling technology, design guideline or tool that requires further distribution to enhance the Foundation's safety and health agenda as a result of this project.

No publications have been submitted at the time of this writing. However, one paper is in preparation for submission to the *Journal of Aerosol Science* and two others are being prepared for publications as *ASME-DSCC* papers.

6.0 Conclusions and Impact Assessment: The report must provide concise and clear conclusions derived and supported by the research findings. A key goal of the Foundation's agenda for funding these research efforts is to produce practical outputs that have a measureable impact on mining health and safety. In this context, the report should also draw conclusions regarding how and to what degree the project accomplishments advanced the science, solved the problem that was the topic of the research grant and/or can guide practical applications that are likely to improve mining safety and health.

The research conducted during the course of this grant demonstrated that fog can improve the scavenging of nanoparticles in two different testing environments. In a laboratory environment testing sodium dodecyl sulfate (SDS) nanoparticles, the research demonstrated that fog having a number density on the order of $10^{12}/m^3$ (10^6/cc) improved the scavenging coefficient by about 30%, a number that varies with volumetric flow rate and particle diameter, as detailed in this report. The agglomeration coefficient, K was increased by as much as an order of magnitude. The laboratory test results showed that the drop number density is the driving factor in the degree to which fog improves K.

In the engine test-cell environment, the less controllable environmental conditions made difficult the quantification of the improvement of both E and K due to fog. The results in the form of time traces show that improvement is there. However, spurious results and fluctuations in the number density of particles can mask this effect. This notwithstanding it appears that a 5% to 15% increase in E occurs in the presence of fog. For K, an increase between 15% and 25% is observed for total DPM over all particle diameters measured. The PIs feel that these numbers would increase in an environment with less variability. We also note that the challenges in *quantifying* E and K are significant, though building and operating an fog scavenging system is significantly less difficult.

Broadly state, the research presented here shows that for fog number densities on the order of $10^{12}/m^3$ (10^6/cc), significant improvement in nanoparticle scavenging can be attained. Many factors affect both E and K, including flow speed, particle diameter, and likely others that were not explored in this research. Nevertheless, in two fairly different environments, these results suggest that it is the drop number density that is the critical parameter to ensure the removal of DPM from diesel exhaust. The challenges, as detailed below in Future Work, is in developing the methods to ensure high fog number density generation. Using the method for fog generation explored here, this is a challenge. Even under ideal circumstances, the ultrasonic foggers employed here produced this drop number density only under low exhaust flow rates (or air flow rates in the laboratory experiments), However, in the presence of diesel, significant modifications of the setup were necessary to ensure that fog generation did not cease due to contamination of the water surface by hydrocarbon films. All of this notwithstanding, these results suggest that regardless of exhaust flow rate, implementation of a fogging system capable of generating fog number densities of $10^{12}/m^3$ (10^6/cc) should enable significant DPM scavenging from the tailpipes of mining vehicles.

One result of this work, though not presented in the form of tables or plots, is that thermal issues are not a significant impediment to the use of a fog scrubber. Prior to conducting this research, there was concern that the high temperatures of diesel exhaust might serve to evaporate fog drops, eliminated any possible utility of fog. However, this research showed that a simple shell and tube heat exchanger can bring the exhaust down to room temperature.

Finally, it is noted that an important lesson learned from this research is building a prototype fog scrubber that removes diesel particles is not a difficult task. However, building an experimental setup that can measure the improvement is a significant challenge. Changes in engine operating condition that seem to be common, result in significant changes in many aspects of DPM production, to the point that the effect of fog can be obscured.

7.0 Recommendations for Future Work: Recommendations for future work shall be summarized.

The results presented here suggest that the following research/development steps are the appropriate paths forward to enable implementation of fog scrubbers on diesel-powered mining vehicles.

(1) Development or procurement of foggers capable of generating high number density fog in dirty environments.

(2) Development or procurement of foggers that are robust to contamination due to oil films or films due to other hydrocarbons found in diesel exhaust.

(3) Engineering development of systems that enable recirculation of the water used, including filtration methods to ensure that diesel that is scrubbed out of the exhaust does not get reintroduced when the water is reused for fog generation and which can be run for long durations so as to avoid the need for frequent filter replacement.

(4) Though a heat exchanger was very effective in cooling exhaust down to room temperature, enabling fog to do its job in terms of scrubbing, in the experiments completed in this work, this heat exchanger was always used in a once through mode, where tap water flowed through the liquid side of the heat exchanger and then went to drain. Development of a simple radiator system that would close the loop on the water side of the loop would be an important step forward.

(5) Future work on *quantifying* the effect of a fog scrubber on diesel exhaust should be conducted on an engine that is outfitted with closed loop control over rpm and engine load, and perhaps other variables as well. Significant time spent ensuring that an engine can be operated in a steady-state condition is recommended.

8.0 References: List all relevant references cited in the Final Report that support the research effort.

Brandon, C.N. (2012). "Emerging Workforce Trends in the U.S. Mining Industry," Automated Systems Alliance Inc., for the SME, NMA, NSSGA, and IMA-NA, 2012, Society for Mining, Metallurgy and Exploration, Englewood, CO.

Bugarski, A. D.; Schnakenberg, G. H.; Patts, L. D. (2006). "Implementation of diesel particulate filter technology in underground metal and nonmetal mines," Proceedings of the Eleventh U.S./North American Mine Ventilation Symposium, University Park, PA, June 5-7. Taylor & Francis Group, pp. 127-133.

Bugarski, A. D.; Schnakenberg, G. H.; Hummer, J. A.; Cauda, E.; Janisko, S. J.; Patts, L. D. (2009). "Effects of diesel exhaust after-treatment devices on concentrations and size distribution of aerosols in underground mine air," Environ. Sci. Technol., 43, pp. 6737-6743.

Bugarski, A. D.; Janisko, S. J.; Cauda, E. G.; Noll, J. D.; Mischler S. E., (2011). "Diesel aerosols and gases in underground mines: guide to exposure assessment and control," DHHS (NIOSH) Publication No. 2012-101.

Bugarski, A. D.; Janisko, S. J.; Cauda, E. G.; Noll, J. D.; Mischler, S. E. (2012). "Controlling Exposure to Diesel Emissions in Underground Mines," Society for Mining, Metallurgy, and Exploration, Inc., Englewood, CO.

Cheng, L. (1973). "Collection of Airborne Dust by Water Sprays," Journal of Industrial and Engineering Chemistry Process Design and Development, 12(4), pp. 221-225.

Colinet, J. F.; Flesch, J. P. (1997). "Exposure to silica dust on continuous mining operations using flooded-bed scrubbers," NIOSH, NIOSH Publication No. 97-147.

Colinet, J. F.; Thimons, E. D. (2002). SME Annual Meeting, Feb 25-27, Phoenix, Arizona, Preprint 02-189. Littleton, CO: Society for Mining, Metallurgy, and Exploration, Inc., Feb, 1-6.

Cooper, C. D.; Alley, F. C. (1994). "Air Pollution Control," Waveland Press, Inc., Prospect Heights, IL.

Dementhon, J.; Martin, B. (1997) "Influence of various diesel traps in particulate size distribution," SAE Technical Paper, No. 972999.

Dockery, D. W.; Pope, C. A.; Xu, X.; Spengler, J. D.; Ware, J. H.; Fay, M. E.; Ferris, B. G.; Speizer, F. E. (1993). "An association between air pollution and mortality in six U. S. cities," J. Medicine, 329, pp. 1753-1759.

Elder, A.; Gelein, R.; Silva, V. et al. (2006). "Translocation of inhaled ultrafine manganese oxide particles to the central nervous system," Environ. Health Oerspect., 114, pp. 1172-1178.

EPA (1999). "Air quality criteria for particulate matter, Vol. II," EPA document 600/P-99/002b.

EPA (2002). "Health Assessment Document for Diesel Engine Exhaust, Prepared by the National Center for Environmental Assessment for the Office of Transportation and Air Quality," Washington, DC.

EPA (2009) "Diesel oxidation catalyst general information," EPA Technical Bulletin.

NIOSH, DHHS (2012). "Coal Mine Dust Exposures and Associated Health Outcomes: A Review of Information Published Since 1995," Publication No. 2011–172.

CDC (2006). "Advanced Cases of Coal Workers' Pneumoconiosis-Two Counties, Virginia," MMWR, 55(33).

Federal Register (2014). “Lowering Miner’s Exposure to Respirable Coal Mine Dust, Including Continuous Personal Dust Monitors; Final Rule, 79,” Fed. Reg. 24813.

Esswein E. J.; Breitenstein M.; Snawder, J.; Kiefer, M.; Sieber, W. K. (2013). “Occupational exposures to respirable crystalline silica during hydraulic fracturing,” J Occup Environ Hygg ;10(7), pp. 347-356.

Greenberg, M. I.; Waksman, J.; Curtis, J. (2007). Silicosis: a review. Dis Mon, 53, pp. 394-416.

Greenfield, S. M. (1957). “Rain Scavenging of Radioactive Particulate Matter from the Atmosphere,” Journal of Meteorology, 14, pp. 115–125.

Hartma,n H. L.; Mutmansky, J. M.; Ramani, R. V.; Wang, Y. J. (1997). Mine ventilation and air conditioning, Third Edition. New York: John Wiley & Sons, Inc.

Hinds, W. C. (1982). Aerosol Techology, John Wiley & Sons, Inc., New York.

Howell, S.; Weber, A. J. (1997). "Biodiesel use in underground metal and nonmetal mines," DieselNet Technical Report.

ICRP Task Group Model (1984) Ann. Am. Conf. Ind. Hyg., 11.

Kim, H. T.; Jung, C. H.; Oh, S. N.; Lee, K. W. (2001). “Particle Removal Efficiency of Gravitational Wet Scrubber Considering Diffusion, Interception, and Impaction,” Environmental Engineering Science, 18(2), pp. 125–136.

King, L. V. (1934). “On the acoustic radiation pressure on spheres,” Proceedings of the Royal Society of London. Series A-Mathematical and Physical Sciences, 147(861), pp. 212-240.

Kissell, F. N. (2003) Handbook for Dust Control in Mining, DHHS (NIOSH) Publication No. 2003-147, IC 9465.

Kittelson, D. B. (1998). "Engines and nanoparticles: a reiew," J. Aerosol Sci., 29 (5/6) pp. 575-588.

Kittelson, D. B.; Watts, W. F.; Johnson, J.P.; Rowntree, C.; Payne, M.; Goodier, S.; Warrens, C.; Preson, H.; Zink, U.; Ortiz, M.; Goersmann, C.; Twigg, M. V.; Walker, A. P.; Caldow, R. (2009). "On-road evaluation of two diesel exhaust aftertreament devices," Journal of Aerosol Science, 37, pp. 1140-1151.

Lapple, C. E. (1951) "Processes use many collector types,: Chemical Engineering, 58(5).

Licht, W. (1984). "Control of Particles by Mechanical Collectors," in Handbook of Air Pollution Technology, S. Calvert and H. M. Englund, Eds., John Wiley & Soncs, Inc., New York.

Mischler, S. E.; Colinet, J. F. (2009). "Controlling and monitoring diesel emissions in underground mines in the United States," Proceedings of the Ninth International Mine Ventilation Congress, New Delhi, India, Nov. 10-13, Oxford & IBH Publishing Co. Pvt. Ltd., pp. 879-888.

Mischler, S. (2014) “A Multistage Cyclone Array for the Collection of Size-segregated Silica Aerosols to Test the Hypothesis that Ultrafine Crystalline Silica Particles are More Efficient in Their Activation of Macrophages.” Doctoral Dissertation, University of Pittsburgh.

Maricq, M. M.; Chase, R. E.; Xu, N.; Laing, P. M. (2002) "The effects of the catalytic converter and fuel sulfur level on motor vehicle particulate matter emissions: light duty diesel vehicles," Environ. Sci. Technol., 36, pp. 283-289.

T. M. Merrell, T. M.; Saylor, J. R. (2017) “Scavenging of micron-scale particles using a combination of fog and a cylindrical ultrasonic standing wave field,” J. Aerosol Sci. vol. 107, pp. 14 - 30.
MSHA (2013). “Quantitative Risk Assessment in Support of the Final Respirable Coal Mine Dust Rule,” Available: http://www.msha.gov/endblacklung/docs/Quantitativeanalysis.pdf (accessed Feb 10, 2015).

NIOSH (1988). “Carcinogenic effects of exposure to diesel exhaust,” DHHS (NIOSH) Publication No. 88-116, Current Intelligence Bulletin 50.

Oberdorster, G.; Sharp, Z.; Atudorei, V.; et al. (2004). "Translocation of inhaled ultrafine particles to the brain," Inhal. Toxicol., 16, pp. 437-445.

Oberdorster, G.; Oberdorster, E.; Oberdorster, J.; (2005). "Nanotoxicology: an emerging discipline evolving from studies of ultrafine particles," Environ. Health Perspect., 113, pp. 823-839.

Oberdorster, G.; Stone, V.; Donaldson, K. (2007). "Toxicology of nanoparticles: a historical perspective," Nanotoxicology, 1, pp. 2-25.

Page, S. J.; Organiscak, J. A. (2000). “Suggestion of a Cause-and-Effect Relationship Among Coal Rank, Airborne Dust, and Incidence of Workers' Pneumoconiosis,” Am Ind Hyg Assoc J, 2000 Nov-Dec 61(6) pp. 785-787.

Pollack, D.; Organiscak, J. (2007). “Airborne Dust Capture and Induced Airflow of Various Spray Nozzle Designs,” Journal of Aerosol Science and Technology, 41(7), pp. 711-720.

Pope, C. A.; Thun, M. J.; Namboodiri, M. M.; Dockery, D. W.; Evans, J. S.; Speizer, F. E.; Heath, C.W. (1995). "Particulate air pollution as a predictor of mortality in a prospective study of U. S. adults," Am. J. Respir. Crit. Care. Med., 151, pp. 669-674.

Ran, W.; Saylor; J. R.; Holt, R. G. (2014). “Improved particle scavenging by a combination of ultrasonics and water sprays,” Journal of Aerosol Science, 67, pp. 104-118.

Ran, W.; Saylor, J. R. (2015a). "The directional sensitivity of the acoustic radiation force to particle diameter", J. Acoust. Soc. Am. vol. 137, pp. 3288-3298.

Ran, W,; Saylor, J. R. (2015b) "A mechanistic explanation of the increase in particle scavenging in the ultrasonic scrubber," J. Aerosol Sci. vol. 87, pp. 88-101.

Ristovski, Z. D.; Miljevic, B.; Surawksi, N. C.; Morawska, L.; Fong, K. M.; Goh, F.; Yang, I. A. (2012). "Respiratory health effects of diesel particulate matter," Respirology, 17, pp. 201-212.

Schnakenberg, G.H.; Bugarski, A. (2002). "Review of technology available to the underground mining industry for control of diesel emissions," DHHS (NIOSH) Pubication No. 2002-154.

Seaton, A.; MacNee, W.; Donaldson, K.; Godden, D. (1995). "Particulate air pollution and acute health effect," The Lancet, 345, pg. 177.

Serrano, J> R.; Climent, H.; Piqueras, P.; Angiolini, E. (2014). "Analysis of fluid-dynamic guidelines in diesel particulate filter sizing for fuel consumption reduction in post-turbo and pre-turbo placement," Applied Energy, 132, pp. 507-523.

Shepherd, C. B.; Lapple, C. E. (1939). "Flow pattern pressure drop in cyclone dust collectors," Industrial and Engineering Chemistry, 31(8).

Smoluchowski, M., Phys. Z. vol. 17, pp. 557 (1916).

Smoluchowski, M., Z. phys. Chem. vol. 92, pp. 129 (1918).

Stairmand, C.J., "The Design and Performance of Cyclone Separators", Transactions of Industrial Chemical Engineers, vol. 29, pp. 356-383, 1951.

Vaaraslahti, K.; Virtanen, A.; Ristimaki, J.; Keskinen, J. (2004). "Nucleation mode formation in heavy-duty diesel exhaust with and without a particulate filter," Environ, Sci. Technol., 38, pp. 4884-4890.

Vogt, R.; Scheer, V.; Casati, R. Beter, T. (2003). "On-road measurement of particle emission n the exhaust plume of a diesel passenger car," Environ. Sci. Technol., 37, pp. 4070-4076.

Warheit, D. B.; Seidel, W. C.; Carakostas, M. C.; Hartsky, M. A. (1990). "Attenuation of perfluoropolymer fume pulmonary toxicity: Effect of filters, combustion method, and aerosol age," Pulmonary Toxicity of Perfluoropolymer Fumes. Academic Press, NY, pp. 309-329.

Watts, W. F. Spears M.; Johnson, J. (1998). "Evaluation of biodiesel fueld and a diesel oxidation catalyst in an underground metal mine," Diesel Emissions Evaluation Program (DEEP) Report.

9.0 Appendices: Include any material that cannot be conveniently or logically included in the body of the report that is relevant to support the effort or outcome of the project accomplishments or conclusions. For example, data sets that support the research approach and the record of accomplishments can be provided in the Appendix.

N/A